University of Illinois at Urbana-Champiagn

ME 470: Senior Design

Design of a Solar Desalination System

Final Design Report

December 16, 2021

Authors:

John Clancy johnwc2@illinois.edu
https://www.overleaf.com/project/619d742801dd0d9581de9a09 Ian Honeywell imh2@illinois.edu
Maxwell Shaw mtshaw2@illinois.edu
Jacob Wojtasik jacobpw2@illinois.edu
https://www.overleaf.com/project/619d742801dd0d9581de9a09

Faculty Advisor:
Prof. Quinn Brewster

TA:
Amir Chavoshi

Submitted To:
Prof. Jont Allen
ECE, University of Illinois
3062 Electrical & Computer Eng. Bldg.
Urbana, IL 61801

Contents

List of Figures

List of Tables

1 Executive Summary

In the interests of combating water scarcity around the globe, Prof. Jont Allen developed a system that simulates the use of solar energy in the desalination of ocean water.

Over the course of the Fall 2021 semester, the system was tested and improved upon. Initial design alterations were motivated by the need to model and test the system; these design alterations enhanced the ability of the system to measure and control state variables. The existing LabVIEW measurement system was improved upon by replacement with Adafruit thermocouples connected to an Arduino/Raspberry Pi system. Additionally, water level measurement was automated using a USB-camera and the python OpenCV module. Controls were put in place for water inflow rate. The water collection chamber of the system was redesigned in acrylic to improve the experimental accuracy of the system and allow modeling of the condenser system. Final design alterations made smaller changes to the system, such as exchanging the 33 LPM air pump out for a larger, 66 LPM air pump. In total the design changes cost \$1,058.33 of the \$1,500, with the highest cost involving the production of the new water collection chamber.

Thermodynamic modeling was performed concurrently with the design changes of the system. The system model is divided up into two separate models, which model the evaporation chamber and the condensation chamber. The modeling process was used to plan experiments for the system. Experiments were run throughout the semester, and mostly varied the water inflow rate to the system with the goal of creating steady-state conditions within the evaporation chamber (and thus keeping the water level constant). The experiments were used to verify the models, and the models were used to explain how the system works, and where there is room for improvement.

The overall goal of driving the evaporation chamber to steady-state has been achieved; however, in the pursuit of optimizing the evaporation chamber, the condensation process is mostly left untouched, and so it is a bottleneck to the system. Additionally, other research over the course of the semester has fueled some recommendations for future semesters that are tackling this project, who will likely be continuing work with the now-improved system. These recommendations involve increasing system measurement and control devices, adding saltwater and solar power, and fixing issues with the system.

2 Introduction

Over the past 100 years, the climate of the Earth has been steadily rising due to the phenomenon known as "global warming".[4] Climate change contributes to a multitude of other issues such as habitat destruction, more extreme weather conditions, and water scarcity. Our sponsor, Professor Jont Allen, who is part of the ECE department at the University of Illinois at Urbana-Champaign, was inspired to tackle the issue of water scarcity because there is, in fact, a large supply of water; however, the vast majority of the water on the planet is undrinkable seawater. In this pursuit, Prof. Allen tasked us with designing and testing a system that uses solar energy to desalinate ocean water.

Previous semesters of ME470 groups approached this task and offered their own solutions, and performed their own research. Over the summer of 2021, Professor Allen built off of the ideas and discoveries of the prior groups and created a working system for use in this semester of ME470. The system designed by Professor Allen evaporates simulated seawater into water vapor, then condenses the vapor into pure water, with the process being fueled by simulated solar energy. The system was improved upon and used for research this semester, and this report serves as a summary of all the work done with the system from August 2021 to December 2021.

2.1 Problem Statement

The original solar desalination system needs design improvements to reach quasi-steady-state for experimental research and modeling purposes.

2.2 Project Objectives

1. Reaching the steady state of the system by matching the evaporation and condensation rates

2. Implementing design changes to increase the accuracy and precision of experiments conducted

3. Develop a thermodynamic model of the system and verify it using experimental results

2.3 Literature Review

To understand the various concepts and current methods surrounding this project a review of academic sources pertaining to solar energy, thermodynamics, and heat transfer was conducted. This research consisted of reviewing academic textbooks, scholarly articles, and previous experiments to understand the principles of this project. This research provided a basis of understanding of solar energy, areas of design to investigate, and how to model the system in order to achieve the goal of determining and modeling the steady state of the system.

To understand the power source of the system a review of solar energy principles was conducted. This review found that solar energy is a carbon-free renewable energy solution that has the most abundant source in the world. [5] The earth is exposed to 170,000 TW of solar radiation at any given time, [1] and the average amount of solar irradiance that passes through the Earth's atmosphere is about 342 W*m-2. This is also the average in a day, so the value is doubled at a location during the day and is zero at night. Given an average of about 600 W*m-2, it is possible to assume 500 W of solar energy strike each square meter of the Earth's surface for around 5 to 8 hours in a day. As seen in Figure 1, higher solar irradiance is recorded near the equator because the sun, on average, points toward the equator. [5] In areas of the ocean closer to the equator, the water's surface can heat up to about 25^{o}C. With the assistance of the evaporation chamber, the sun has enough energy to heat the water to 40^{o}C. Solar photovoltaic panels and an energy storage system could provide additional support to maintain an energy concentration of 500 W*m-2 by collecting extra energy from the sun and using it to power heaters during the night.

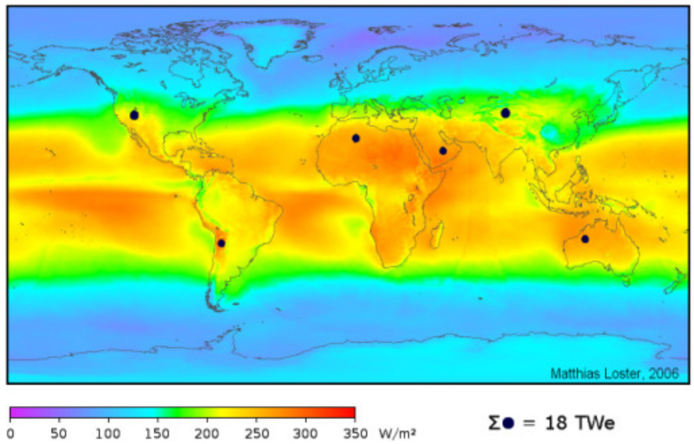

Figure 1. [1] Annual Average Solar Irradiance Across the Surface of the Earth

To determine design changes an analysis of the evaporation chamber design was needed, with the first area of analysis being the water stones used to increase evaporation. In Wang et al [6] small water droplets were studied to determine how droplet size, temperature, and humidity affect the evaporation and movement characteristics of the water. The temperature was adjusted from 298K-353K (roughly 25 °C - 80 °C), the relative humidity ranged from 0-80 percent, and the droplet size varied from 20-80 µm. Throughout testing it was shown that an increase in temperature, a decrease in droplet diameter, and a decrease in relative humidity expedited the evaporation rate. The studied concluded that the three factors all contributed to evaporation characteristics and showcased dependent behavior to each other. This aided our project in determining that more air bubbles of smaller diameter, increased heat, and a decrease of humidity in the evaporation chamber was needed. These changes were implemented by adding more air stones with smaller diameter bubbles, moving the thermometer out of the evaporation chamber water to increase the water temperature, and adding a fan system to pull the water vapor out of the evaporation chamber to decrease humidity. These are discussed in further detail in the Design Alterations section below.

An investigation of evaporation methods for desalination was also conducted to determine if the heat source and plastic evaporation chamber needed to be changed. In Jaakkola [7] plastic evaporators were tested for possible use in saltwater desalination. The article argued that a high cost of desalination is the extensive evaporators needed for multiple stage evaporation. The experiment evaluated the physical strength and evaporation characteristics of the AQUAMAX MC plastic evaporator. The study concluded that the plastic evaporators far exceeded the necessary strength and heat transfer requirements for saltwater desalination. Additionally, the plastic provided resistance against corrosion from the saltwater and could be scaled effectively due to low cost of manufacturing.

Peng Tao [3] and his colleagues propose a more efficient way to evaporate seawater by heating the surface of the water instead of the tradition bottom heating. A carbon-based or plasmomic-based material would be placed on the surface of the water acting as a black body. This would heat the surface of the water and evaporation would occur between small openings within the material. This would minimize thermal loses improve energy conversion efficiency compared to bottom heating. This heating method is outside of the scope of this semester's goal of achieving the steady state of the system, but is an important improvement to explore for scaling purposes after steady state is achieved.

Another major design challenge was how to best measure the water level of the evaporation chamber. Tim Shedd's [2] master dissertation includes the idea of using diffused light that is refracted and reflected over a plastic, water, and air interface to measure water depth. This method can prove to be useful within 10 microns for determining the depth of the water for the purposes of determining evaporation rate, water flow rate into the tank, and the steady state of the system. If the variation of the volume of water in the tank is near constant with water flowing into the evaporation tank and vapor flowing outside of the tank, then steady state of the system is presumably achieved. Having the volume of water constant within 10 microns would prove this. This was a viable design idea and lead to the exploration of a computer measurement system as discussed in the Design Alterations section.

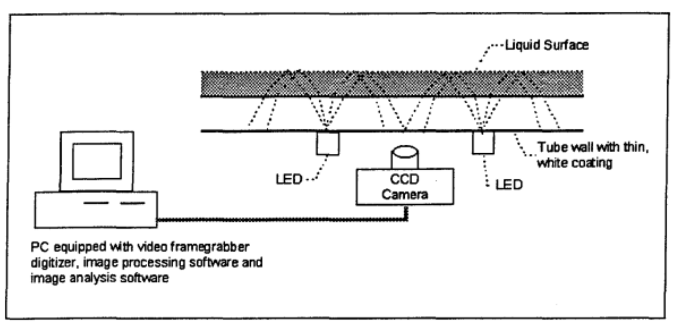

Figure 2. [2] Method of capturing water depth using laser refracted and reflected through a glass, water, and air interface captured by a camera

The next two papers being reviewed are by Abdel Dayem[8] and by Al-Kharabsheh [9]. They discuss the creation and modeling of solar desalination systems similar to the one proposed in this report. In Abdel Dayem, their condensation chamber was directly above the evaporation chamber; water was heated either via a solar collector or a small heater, and the water was vaporized via forced convection through nozzles. Water vapor was condensed onto the condensation chamber walls, which were cooled by ambient air. The paper defined their system efficiency as the ratio of the latent energy of the condensed desalinated water to the total power input, which is the inspiration for our system efficiency as is discussed in Section 6.2. In this respect, they used heat balance of the condenser surface (an annular cylindrical space) to calculate the efficiency; they calculated the heat transfer coefficient using equation 10.30 in Bergman [10], which assumes laminar film condensation on a vertical plate. While their method does not directly apply to our condenser design, a similar approach to calculating system efficiency and determining the heat transfer in the condenser may yield a reliable model. In their experimental results, they found that condensation ability is not an issue, but evaporation should be promoted because that is the limiting factor in the design. Other relevant results include the fact that they best way they improved system efficiency was by increasing water temperature, experiencing a rise from 43% to 63% when water temperature was increased from 75 °C to 97 °C. For our system, the limiting factor is the condensation process; evaporation occurs at a much higher rate than the condenser can handle. This suggests that a simpler or more effective condenser system may be the key to improving the system. This is discussed further in the conclusions and recommendations, Section 8.

Al-Kharabsheh [9] proposes and analyzes a solar distillation system, consisting of an evaporation chamber connected to a pure water chamber via a slanted tunnel lined with condenser fins. Saltwater was injected into the evaporator tank, while concentrated brine was withdrawn from the tank. In order to model their system, they applied mass, energy, and salt balance equations for the whole system, and then analyzed the condenser system. For their condenser analysis, they used heat balance on the condenser surface, modeling the condenser as a horizontal tube with circular fins. They considered both conduction through the condenser wall, and convective heat transfer from the fluid. Heat transfer coefficients were calculated using existing equations for the circular fin design. They solved their system of equations using a finite difference method and defined their efficiency as the ratio of the energy used to evaporate the water to the solar energy input to the system; in a way this quantifies the efficiency of the solar panel as a power source, which is something that was not explored in our project, given that power is provided by a 500 W heater. Their whole-system approach with analysis of individual systems is a very useful basis for our modeling; in addition, the paper conducts a similar thermodynamic and heat transfer analysis as Abdel Dayem [8], and hence we may be able to draw from both papers to support our analysis of our own solar desalination system.

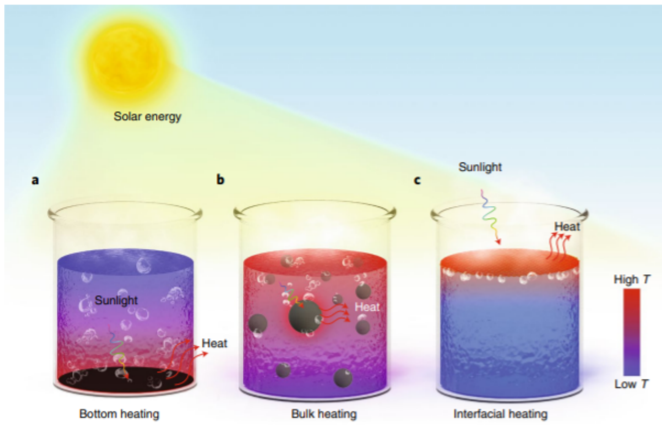

Figure 3. [3] Different concepts of heating a body of water using solar energy

2.4 Project Constraints

The product design specification (PDS) defines the system requirements and constraints. The PDS was created early in the semester to guide the design change and research process. Not all of the elements apply, given the goals of the project; those elements that do apply are highlighted in blue in Fig. 4. Given the experience gained during this semester, some new specifications and suggestions for the future are discussed below.

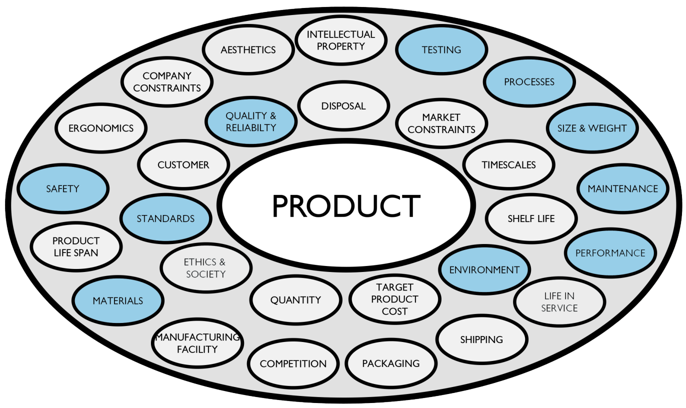

Figure 4. The elements of the product design specification, with the most relevant elements highlighted in blue

Performance: The system must produce water at a reasonable rate for a given amount of power and space. Initially, it was proposed that the system should operate at 60% energy efficiency and produce at least 1 gallon of pure water in an 8 hour period (with the 500 W heat source). The system from the end of the semester operates at lower values than this, and so this goal/constraint should remain.

Environment: The system is set up in the Sidney Lu MEB, which is slightly colder than room temperature at about 19 °C. The air is clean and dry, and the pressure is assumed to be about 1 standard atmosphere. Experiments run during the semester showed that internal environment of the system is also a big consideration. The system operates at temperatures from 35°C to 50°C, with relative humidity ranging from 95% to 100%.

Maintenance: All the components of the system are susceptible to water scale, and hence they should be cleaned weekly. In addition, measurement tools such as the thermistors, should be calibrated before every experiment. Govee hygrometers additionally must be monitored for failure due to the humidity, as this occurred once this semester.

Size: The laboratory setup fits on a 3' x 5' table, with 2' high plastic bins. Additionally, a standard water heater/cooler sits on a table nearby. The system remained within these constraints throughout the semester, and this sizing is found to be reasonable for testing.

Materials: Materials must be able to withstand temperatures as low as 10 °C, and as high as 50 °C. Additionally, it was observed that the insulation used is susceptible to water leakage; this should be accounted for in the future.

Standards & Regulations: Relevant standards include the WHO standards on safe drinking water from desalination, the EPA regulations for water intake systems, and the IEEE photovoltaic standards. These regulations were not explored this semester, but will play a crucial role in developing a product around this system.

Quality & Reliability: The feedback loop system in the evaporation chamber was improved during this semester; it will require more improvements to increase the range of system parameters, such as water temperature. Additionally, heat loss in the system due to poor insulation was quantifiable; this could be a future point of improvement.

Processes: The system is based off the process of evaporation and condensation. In addition, the regeneration of energy is considered throughout the system, especially in the condenser where latent heat of the vapor is used to heat up inlet water. Other processes occurred in the system, which caused deviation of the system from the model; these processes included heating of the input air (via compression in the pump) and convection of room temperature air with the exposed (un-insulated) corners of the chambers.

Testing: Components and subsystems should be tested to ensure that they are working and creating the desired effect; any faulty components or insulation could ruin experiments and create variation from the theoretical model. Results from the semester showed that each component of the system should be tested individually to consider its impact on the system. For example, it is critical that the condenser be tested in an isolated environment to determine its effectiveness or other heat transfer characteristics.

Safety: Lots of electrical equipment are being used with hard water, which is a potential hazard. The system operates under moderate temperatures, but standard atmospheric pressures. Feedback loops are being relied on to keep the system from burning or flooding while experiments are run.

2.5 System Overview

The schematic for the design of the system can be seen in Figure 5, and an image of the system prototype can be found in Figure 6. Additional close-up photos can be found in Appendix G. A water cooler is used as the simulated version of ocean water with an average water temperature of 12ºC, which is consistent with an ocean water temperature of 10ºC to 12ºC. The water passes through tubing with with shut off valves, an electric solenoid valve, needle valve, and a rotameter to restrict and measure the water inflow into the system. The cold water enters into the condenser-fan heat exchanger system where it is used to condense the water vapor present inside the condensation chamber. Once the water exits the condenser, its temperature has risen to about 35ºC when it enters the water reservoir inside the evaporation chamber. The water inside the evaporation chamber is additionally heated by the 500 W heater that simulates the solar energy that is incident on the Earth's surface, and the copper coil heat exchanger that uses the increased air temperature from the larger air pump to transfer extra energy before the air is introduced into the air stones underwater in the evaporation chamber. The air introduced by the air stones increases the evaporation rate so more water can become water vapor at a temperature of about 40ºC and the air flow rate is measured by a rotameter. Once the the water is water vapor, a fan near the vents of the condensation chamber pulls the vapor through, coupled with natural diffusion, into the condensation chamber. The condenser-fan system then pulls the humid air and condenses it into potable water in the water collection chamber. The water then drains out of the water collection chamber outlet into a measurable container. Temperatures throughout the system are measured by thermocouples connected to an Arduino processor and a Raspberry Pi microcomputer. Additionally, the humidity and temperatures of each chamber is measured by GoVee hydrometers. The water level of the evaporation chamber is measured by a camera that periodically takes pictures throughout experimental testing.

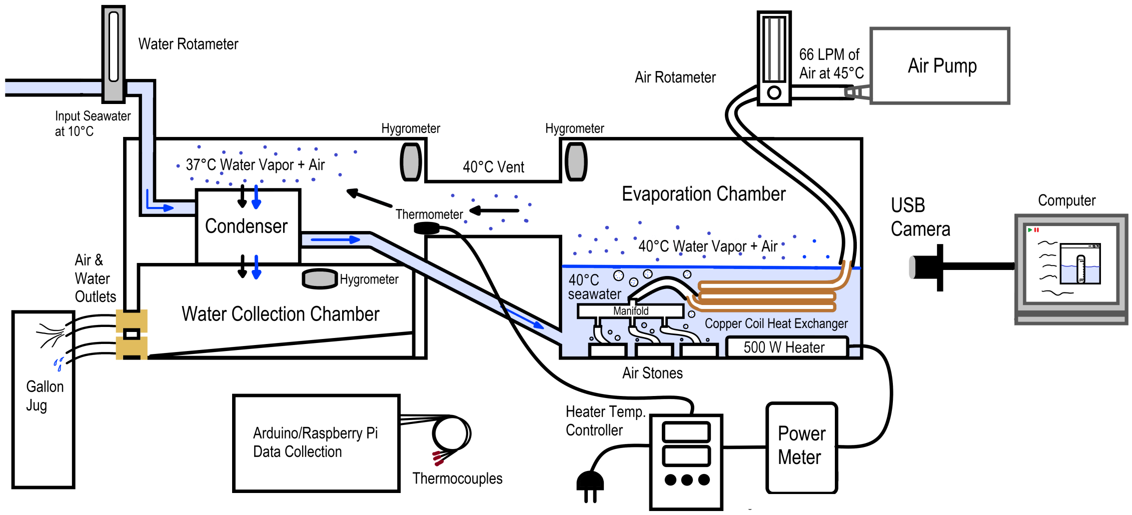

Figure 5. Full schematic of the system as of December 7th

3 Design Alterations

3.1 Initial System Prototype

Over the Summer 2021 semester the project sponsor, Prof. Allen, made various changes to the prototype developed by previous semester. These changes included switching the heat source for the evaporation chamber from a heat lamp, which was meant to mimic direct solar energy, to a 500W submersible heater that mimics the amount of energy produced by the solar panels from direct solar energy. The vents which allow for the saturated water vapor to move from the evaporation chamber to the condensation chamber were enlarged. The air introduced to the evaporation chamber was changed from a laminar airflow across the evaporation chamber to air stones submerged in the evaporation chamber which crated bubbles in the heated water. However, even with these changes the system was still far from completely operating and running at steady-state conditions.

3.2 Data Collection Systems

The Fall 2021 team was brought in to improve various aspects of the system and run experiments to ideally reach steady state operation. One of the initial problems identified was the data collection system. The system was using a LabVIEW thermocouple module and the sponsor's personal computer to collect measurements of the system. Additionally,

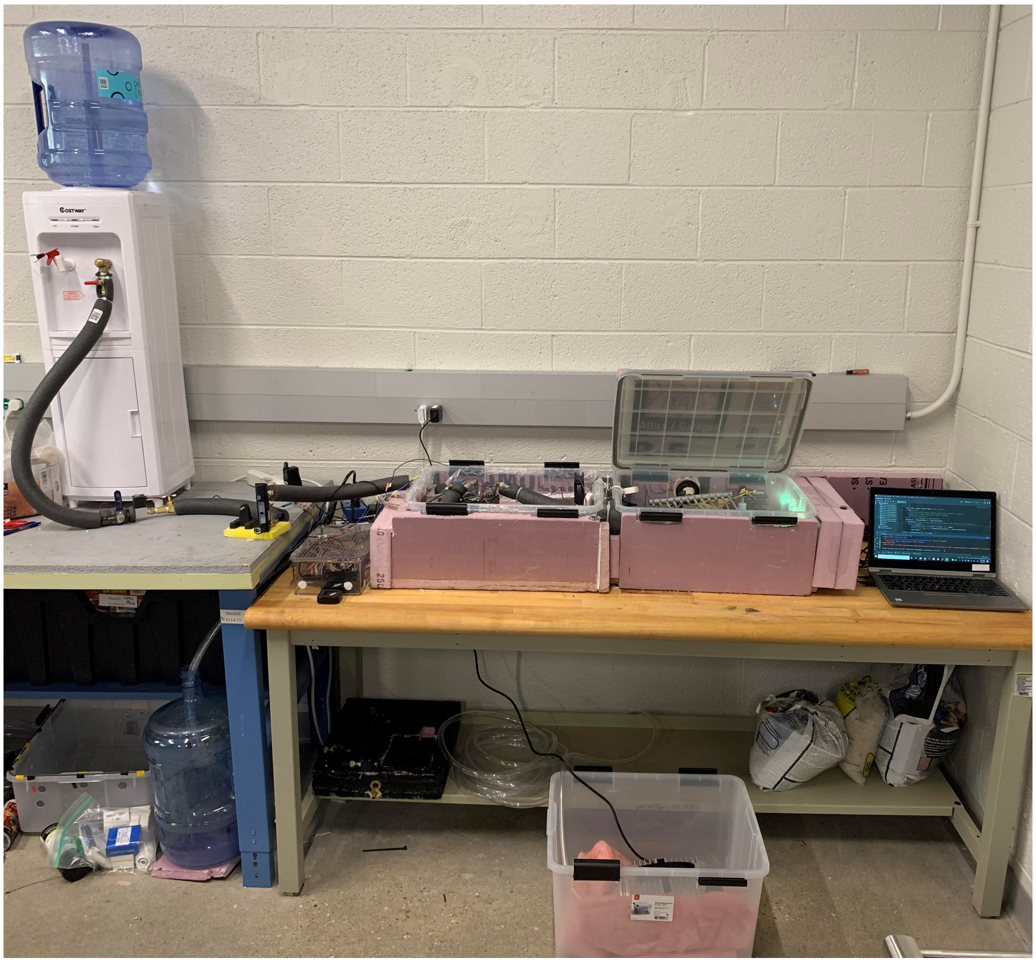

Figure 6. Physical system as of December 7th; close up pictures of the system available in Appendix G

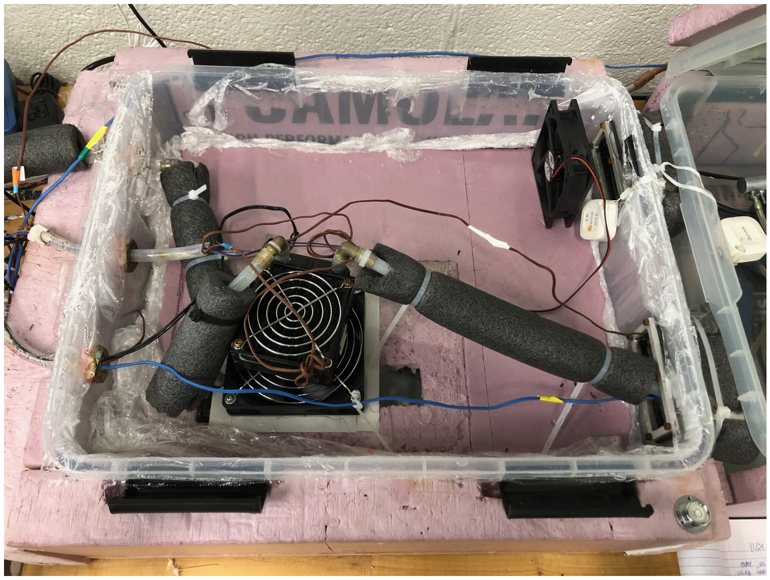

Figure 7. Condensation Chamber

Figure 8. Evaporation Chamber

GoVee hygrometer sensor were used to measure temperature and humidity levels throughout the chambers. The Govee sensors worked well and were left as is. Unfortunately, the LabView data collection system would periodically crash during experiments, and the code to alter the data collection was not in a format the sponsor liked. To improve the data collection system the decision was made to switch the current setup to a Arduino based system. The new system utilized Adafruit thermocouples, Arduino breadboards, a Arduino serial data processor, and a Raspberry Pi to continuously measure the thermocouple data. This allows for the thermocouple data to be more reliable available and to be viewed in real-time from any location. To built this system first the Adafruit thermocouples were assembled via soldering. These thermocouples were then wired into a Arduino breadboard and connected to a Arduino processor. The code to run this sensors was written in an Arduino script and the data could then be viewed on the serial monitor in Arduino. This script did not save the data, so a Raspberry Pi microcomputer was added to this system to allow for data saving and remove the need for a personal computer to be constantly attached to the system. To view the data from the Arduino processor a script was written in the Raspberry Pi terminal to pull the serial data. To enable the data collection to be run remotely a Remote Desktop Connection program was also installed on the Raspberry Pi. Additionally, to save the data a WinSCP file sharing program was installed, which allowed for the data to be easily transferred from the Raspberry Pi to a personal computer in a csv format. To be able to plot this data and make conclusions about experiments a plotting script was written in Python. All of these codes and instructions for how to run the data collection system can be seen in the Appendix.

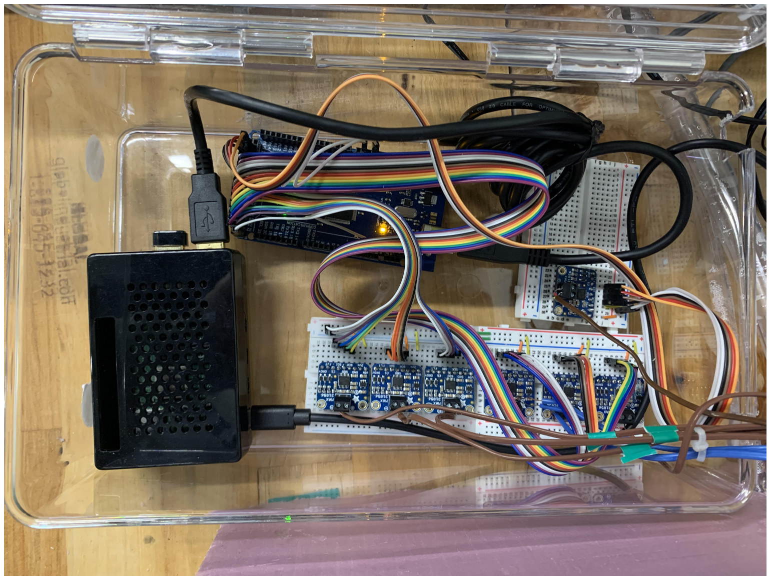

Figure 9. New Data Collection System

3.3 Input Controls and Measurements

In addition to the problems with the data collection, the original system did not have measurements and controls for water and air inputs to the system. There was no control of the water flow into the system and the rate of the water flow was measured by filling a beaker over a time interval. Therefore, the amount of water entering the evaporation chamber could not be adjusted to match the evaporation rate of the heated water. The original water flow rate was 300 mL/min, which was much higher than the initial evaporation rate of 0.673 ml/min. A variable area flow meter was installed, which allowed for a decrease in water flow rate to match the evaporation rate as well as an accurate measurement of water input. The air flow is measured by an air flow rotameter to determine air input into the evaporation chamber. The heat rate is measured by a power meter connected to the heater which provides instantaneous power consumption rates. This allows for calculations of energy input into the system and power measurements of the on and off cycle of the heater.

3.4 Water Level Measurement

In the original system the water level of evaporation chamber was measured by hand with a ruler when experiments were run. This was a problem because the experiments were run over long intervals, which therefore required someone one to come in periodically to take measurements. An autonomous way to measure the water level of the chamber needed to be developed. In order to do this an ELP 3.6mm camera was purchased. This was then connected to a computer running a python code that would capture images periodically throughout the experiment of the water level and a reference ruler. This images were then analyzed using SketchUp Pro 2021, Appendix B, to find the the distance in pixels of the water level change. Additional insulation has been installed to the side of the evaporation tank to house the camera, LED lights, and ruler.

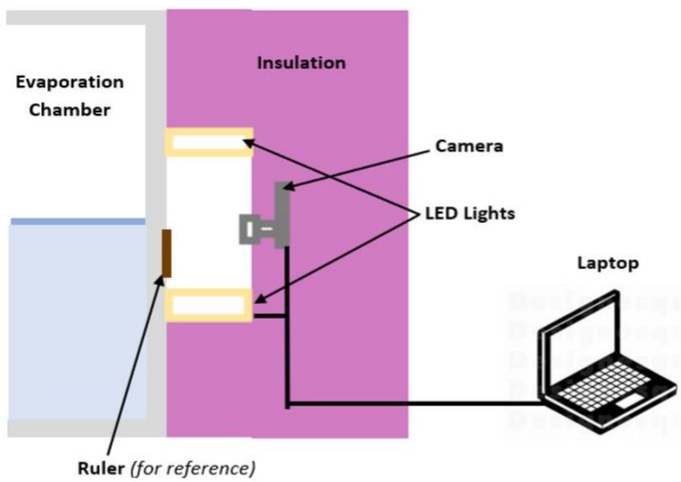

Figure 10. Water Level Camera Setup

3.5 Redesigned Water Collection Chamber

The water chamber was redesigned to prevent the leaking and pooling of water for a more accurate measure of output. The original model was a container made from polystyrene foam insulation. The edges were difficult to seal, so water leaked back into the condensation chamber. Additionally, the water chamber had no sloped decline towards its outlet, so it was difficult to obtain an accurate amount of water in the collection reservoir for measurement. The new chamber was designed in Autodesk Fusion 360 according to the dimensional constraints measured within the condensation chamber. See Figure [3] for a rendering of the new model. It was necessary for the condenser-fan system to remain in the same position within the condensation chamber as before. The original water outlet from the condensation chamber was too high for the water chamber to have an inclined plane while also remaining within its prescribed height constraint, so a new water outlet hole was drilled at a lower height. The new chamber is made of acrylic, which is covered in one inch polystyrene insulation. It contains a V-shaped ramp within the acrylic chamber that funnels down to the water outlet which collects in a jug that can be poured into a beaker to measure water outputs of the system. Also, an air outlet is present at a greater height than water outlet for the air to cycle out of the system.

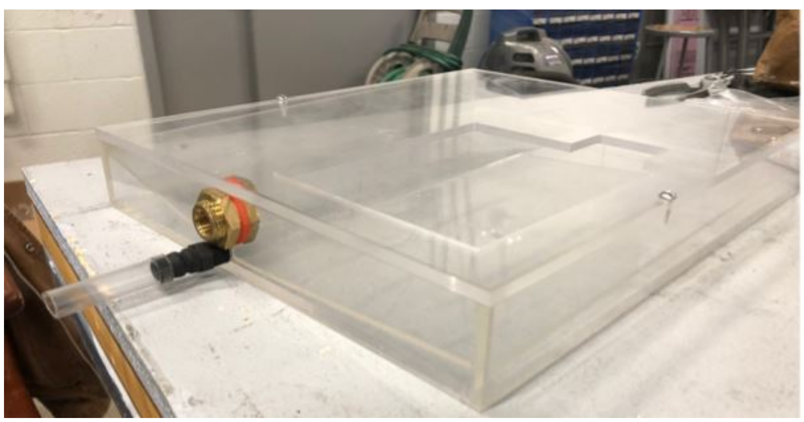

Figure 11. Redesigned Water Collection Chamber

3.6 Larger Air Pump

To increase the evaporation rate of the heated water, a larger air pump was purchased. After the 50 liter/minute air pump was switched out for the 225 liter/minute air pump, the air flow input temperature significantly increased. There was concern that the extra heat from the air input would render the heater obsolete, however the duty cycle of the heat remained the same. Instead, the extra heat was embraced and copper tubing was installed inside the evaporation chamber to create a heat exchanger for another heat flux input.

3.7 Additional Changes

Additional elements that need to be considered in the system design were related to condensation chamber performance and system safety controls. Safety controls in the form of buoy switch actuators were present in the evaporation chamber to shut off the water inflow if the water level in the evaporation chamber rises too high and the heater if the water level falls too low in the initial prototype. However, the wiring of these controls was faulty and made the safety cutoffs unusable. To fix this problem the entire buoy switch actuator circuitry was rewired to ensure the cutoffs would perform reliably during experiments. In later experiments it was found that excess condensation was developing in the condensation chamber outside of the condenser. To combat this problem a fan was added to the vents connecting the evaporation chamber and the condensation chamber to better circulate the air in the condensation chamber.

4 Modeling

Separate models were created to model the condensation and the evaporation processes within the system. Then the evaporation and condensation rate of the separate models were compared.

4.1 Design

The main motivation for creating a theoretical model of the system is to explain how and why the system works, and where there is room for improvement. The models were designed using psychrometry and thermodynamics.

4.2 Introduction

Analysis is performed using concepts taught in the ME200 and ME320 courses. The course textbooks were used extensively; they are *Fundamentals of Engineering Thermodynamics, 8th Ed.* [11], and *Fundamentals of Heat and Mass Transfer, 8th Ed.* [10]

4.3 Changes to Model

Initially, the model was missing various variables which had to be assumed before the proper measuring equipment was introduced. For example, the mass water flow rate through the system was not measured until a rotameter was introduced. Also, the mass inlet air flow rate of the ambient laboratory air was assumed to be the listed flow rate the manufacture provided, until another rotameter was introduced to precisely measure this variable. The temperature of the inlet ambient laboratory air was assumed to be room temperature, until a thermocouple reading determined the air pump was increasing the temperature to above 40°C. This prompted the heater to be useless, so the copper coil tubing heat exchanger was introduced as another heat source into the system. This is modeled using Eqn. 12. The ambient laboratory air was also initially assumed to be dry, but a humdity reading of approximately 29% prompted the moist ambient air to be modeled as a combination of water vapor and dry air entering the system. Lastly, the creation of a new acrylic water chamber allowed for the measurement of water output of the system; this allowed the condenser model to be applied to experiments, as the condensation process was then more reliably controlled and measured.

4.4 Psychrometry

Both models use psychrometry, so it will be discussed outside of and be referenced in both of the models.

4.4.1 Relative Humidity

Relative Humidity is the ratio of the examined water vapor pressure to the theoretical saturated water vapor pressure:

$$\phi = p_v/p_g \tag{1}$$

$$p_v = \text{examined water vapor pressure}$$

$$p_g = \text{saturated water vapor pressure}$$

Given a percentage value from a hygrometer, the pressure of water vapor can be determined to be used for determining the humidity ratio.

4.4.2 Humidity Ratio

The humidity ratio is used to determine the ratio of mass of dry air to water vapor in a moist air mixture using the following equation:

$$\omega = 0.622 \frac{p_v}{p - p_v} \tag{2}$$

$$p_v = \text{examined water vapor pressure}$$

$$p = \text{pressure of mixture}$$

4.5 Evaporation

4.5.1 Overview

Fig. 12 shows the model using the water in the evaporation chamber as the control volume and the parameters that will be discussed.

$$\dot{m}_{Wi} = \text{water mass flow rate in}$$

$$\dot{m}_{Vi} = \text{water vapor mass flow rate in}$$

$$\dot{m}_{Ai} = \text{dry air mass flow rate in}$$

$$\dot{m}_{Ve} = \text{water vapor mass flow rate out}$$

$$\dot{m}_{Ae} = \text{dry air mass flow rate out}$$

$$\dot{Q}_h = \text{rate of heat in from heater}$$

$$\dot{Q}_a = \text{rate of heat in from copper coil heat exchanger}$$

4.5.2 Assumptions

1. Due to water's high thermal conductivity, the temperature of the water in the tank remains constant even with the incoming water temperature and incoming air tem-

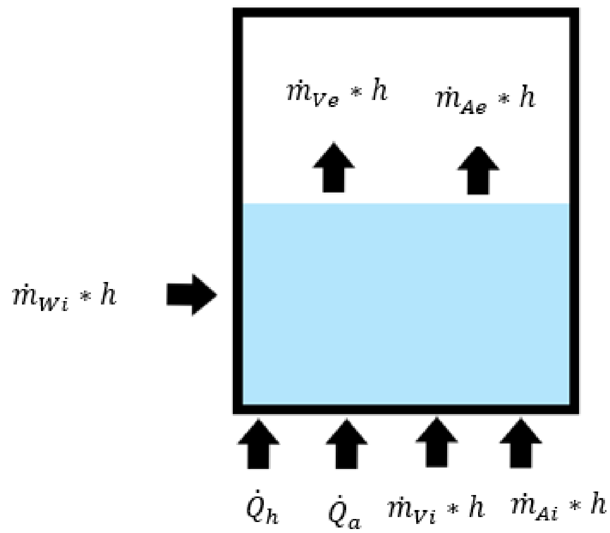

Figure 12. Visual Representation of Parameters for the Steady State of the Evaporation Tank

perature being included into the system. This assumption is explored in greater detail in the next section.

$$T_W = \text{constant} \tag{3}$$

2. Due to the air bubble's high surface area to volume ratio, the temperature of the exiting water vapor is assumed to be equal to the temperature of the water in the tank

$$T_W = T_e \tag{4}$$

3. Additionally from this ratio, the exiting water vapor is assumed to be saturated.

4.5.3 Mass Balance of Control Volume

Since this model is at steady state, the following is true:

$$\sum \dot{m}_i = \sum \dot{m}_e \tag{5}$$

Therefore,

$$\dot{m}_{Ai} + \dot{m}_{Vi} + \dot{m}_{Wi} = \dot{m}_{Ae} + \dot{m}_{Ve} \tag{6}$$

$$\dot{m}_A = \text{mass flow rate of dry air}$$

$$\dot{m}_V = \text{mass flow rate of water vapor}$$

$$\dot{m}_W = \text{mass flow rate of water}$$

Intuitively, it is further known that

$$\dot{m}_{Ai} = \dot{m}_{Ae} \tag{7}$$

$$\dot{m}_{Wi} + \dot{m}_{Vi} = \dot{m}_{Ve} \tag{8}$$

Also, from the humidity ratio, it is known that

$$\dot{m}_V = \omega \dot{m}_A \tag{9}$$

4.5.4 Energy Balance of Control Volume

First, we will begin with the energy balance equation[10]:

$$\frac{dE_{cv}}{dt} = \dot{Q}_{cv} - \dot{W}_{cv} + \sum \dot{m}_i h_i - \sum \dot{m}_e h_e \tag{10}$$

The system is at steady state and no work is being done onto the surroundings due to adequate insulation therefore,

$$0 = \dot{Q}_h + \dot{Q}_a + \dot{m}_{Ai} h_{Ai} + \dot{m}_{Wi} h_{Wi} + \dot{m}_{Vi} h_{Vi} - \dot{m}_{Ae} h_{Ae} - \dot{m}_{Ve} h_{Ve} \tag{11}$$

$\dot{Q}_h$ is the heat rate input from the heater while $\dot{Q}_a$ is the heat rate input from the hot air within the copper tubing. This rate is determined by calculating the enthalpy differences of the air before and after it enters the copper tubing.

$$\dot{Q}_a = \dot{m}_a(h_{Acb} - h_{Aca}) + \dot{m}_v(h_{Vcb} - h_{Vca}) \tag{12}$$

4.6 Condensation

4.6.1 Overview

Two stacked plain straight plate-fin heat exchangers are used in the experimental setup as condensers. Because these heat exchangers are quite similar, they are considered together as one condenser for analysis. A warm, moist air mixture enters into the top of the condenser, where some of the water vapor within is condensed through heat exchange with the working fluid (which is the incoming "seawater"). Moist air and liquid water condensate at lower temperatures then exit the condenser out the bottom. Both fluids are unmixed in the condenser. A simplified diagram of the condenser is show in Fig. 13.

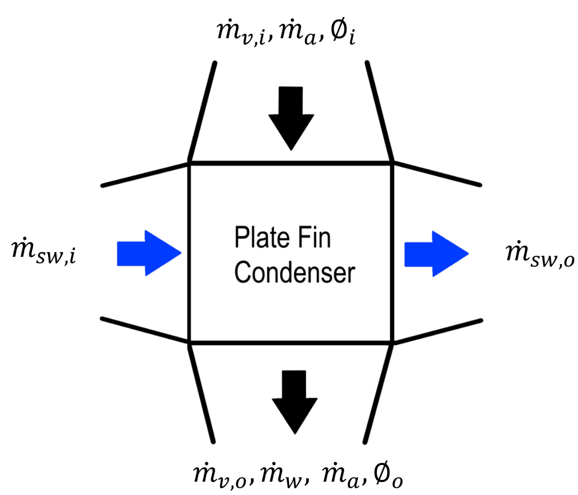

Figure 13. Simplified condenser diagram

4.6.2 Mass Balance

Conservation of mass is applied to the system assuming steady-state conditions. For the simulated seawater, conservation of mass dictates that

$$\dot{m}_{sw,i} = \dot{m}_{sw,o} = \dot{m}_{sw}. \tag{13}$$

For the moist air mixture, conservation of mass is more complicated. Hygrometers are used to measure the temperature and relative humidity of the moist air before and after it passes through the condenser, hence we know the relative humidities ϕ_i and ϕ_o that correspond to humidity ratios ω_i and ω_o. These ratios are calculated using Eq. 2,where the mixture pressure p is assumed to be atmospheric, and the pressure of the water vapor p_v is determined by multiplying saturation pressure at the recorded temperatures times the relative humidity, $p_v = \phi p_g$ (using Table A-2 in *Fundamentals of Engineering Thermodynamics, 8th Ed.* [11]). At steady state, then

$$\dot{m}_{a,i} = \dot{m}_{a,o} = \dot{m}_a \, (dry\, air) \tag{14}$$

$$\dot{m}_{v,i} = \dot{m}_w + \dot{m}_{v,o}. \, (water) \tag{15}$$

The second equation can be rearranged to solve for the condensation rate, $\dot{m}_w = \dot{m}_{v,i} - \dot{m}_{v,o}$. Previously calculated humidity ratios can now be used to simplify this equation, as follows

$$\dot{m}_{v,i} = \omega_i \dot{m}_a \tag{16}$$

$$\dot{m}_{v,o} = \omega_o \dot{m}_a \tag{17}$$

$$\dot{m}_w = (\omega_i - \omega_o)\dot{m}_a. \tag{18}$$

4.6.3 Energy Balance

For the energy balance, some simplifying assumptions must be made for the system. We assume that there is negligible heat loss to the surroundings, and that any changes in potential or kinetic energy of the fluids are negligible. The cold 'seawater' passes into the condenser through tubing; it is assumed that internal flow conditions are fully developed. We assume negligible thermal resistance in the tubing, and negligible fouling effects. Lastly, we assume constant properties for both the water and moist air during the process. Enthalpies of these fluids are only taken to be different at the inlets and outlets of the condenser. The system is assumed to be at 1 standard atmosphere pressure, and water vapor properties are taken at saturation. Lastly assuming $\dot{W}_{cv} = 0$, energy balance for the system gives

$$0 = \dot{m}_{sw}(h_{sw,i} - h_{sw,o}) + \dot{m}_{v,i}h_{v,i} + \dot{m}_{a,i}h_{a,i} - \dot{m}_w h_w - \dot{m}_{v,o}h_{v,o} - \dot{m}_{a,o}h_{a,o} \tag{19}$$

This balance can be represented as a function of *just* the mass flowrates of the working fluid and of the air by substituting in Eqns. 16, 17, and 18:

$$0 = \dot{m}_{sw}(h_{sw,i} - h_{sw,o}) + \dot{m}_a[\omega_i h_{v,i} + h_{a,i} - (\omega_i - \omega_o)h_w - \omega_o h_{v,o} - h_{a,o}]19 \tag{20}$$

Note that in equation 19, the energy associated with the condensate leaving the system can also be written as a combination of the rate of latent heat released by the condensation process (an isothermal process) plus the temperature change of the condensate from the hot temperature down to room temperature, as follows:

$$\dot{m}_w h_w = \dot{m}_w h'_{fg} + \dot{m}_w c_{p,w}(T_{w,o} - T_{v,i}) \tag{21}$$

$$h_w = h'_{fg} + c_{p,w}(T_{w,o} - T_{v,i}), \tag{22}$$

where $c_{p,w}$ is the specific heat of the warm condensed water, and h'_{fg} is the modified latent heat of vaporization of the water vapor, which takes the form

$$h'_{fg} = h_{fg} + 0.68 c_{p,wateratT_{v,i}}(T_{sat} - T_{v,i}). \tag{23}$$

It is also important to discuss how the energy balance is affected by the geometry of the heat exchanger. The effectiveness-NTU method is used in this analysis; firstly, we introduce the heat capacity ratio C_r, which is the ratio of the minimum heat capacity to the maximum heat capacity, as follows:

$$\frac{C_{min}}{C_{max}} = \frac{T_{sw,o} - T_{sw,i}}{T_{v,i} - T_{v,o}} \tag{24}$$

Because condensation is occurring, $C_{max} \to \infty$, and the effectiveness-NTU relationship is outlined for $C_r = 0$ in Table 11.3 in *Fundamentals of Heat and Mass Transfer, 8th Ed.* [10] as

$$\varepsilon = 1 - \exp(\text{NTU}), \tag{25}$$

where ε is the heat exchanger effectiveness, and NTU is the number of transfer units, both defined as

$$\varepsilon = \frac{\dot{Q}}{\dot{Q}_{max}} \tag{26}$$

$$\text{NTU} = \frac{UA}{C_{min}}, \tag{27}$$

where $\dot{Q}$ is the actual heat transfer rate of the heat exchanger, $\dot{Q}_{max}$ is the maximum heat transfer rate of the exchanger, U is the overall heat transfer coefficient of the exchanger, A is the heat transfer surface area, and $C_{min} = \dot{m}_{sw} c_{p,sw}$. The heat exchangers in use in the experiments are simple water-cooling radiators from Amazon, and the only specifications included are that they are pure aluminum fins with a fin density of 18 lines/inch; this is not enough information to determine the number of transfer units or the heat transfer area, so this analysis is not used in the model. It is currently assumed that there is perfect heat transfer from the incoming water vapor to the simulated seawater. However, if the effectiveness of the heat exchanger can be determined, then it can be used in the model to predict how much of the energy is actually transferred between the unmixed fluids.

5 Experiments

Experiments were conducted throughout the semester alongside the continuous system improvements. Often following the same general experimental format, each test provided evidence to the effect of the changes made on the system. The goal was to record the progress being made to achieving quasi-steady-state in the evaporation chamber, and optimizing the system's efficiency and output. Procedures and objectives were recorded in a logbook, and reports were written for each experiment detailing the results, theoretical values, and an analysis based on the original objectives.

5.1 9/25/21 Initial Evaporation Experiment

The first experiment that was conducted was evaluating the evaporation rate of the initial system design created by Prof. Allen. To conduct this experiment the operating procedure found in the Appendix was followed to turn on the system. The evaporation chamber was filled with water until the buoy actuator that turns of the heater was no longer engaged. Next, 5L of water were added to the evaporation chamber and the heater was turned on.

The experiment was left running over a 3.5 day time span with water level and temperature measurements being conducted every 12 hours.

Table 1. Water Level and Temperature Measurements

Time of Measurement	**Water Level Height** (cm)	**Temperature** (°C)
9:38 9/24/21	3.3	30.0
21:02 9/24/21	3.3	40.9
9:39 9/25/21	3.2	40.67
20:30 9/25/21	3.0	40.65
12:13 9/26/21	2.6	41.62
22:15 9/26/21	2.2	40.63
8:41 9/27/21	2.2	40.69
22:18 9/27/21	1.95	40.47
16:01 9/28/21	1.8	40.0

The area of the evaporation chamber was calculated to be 0.1677 m^2. Additionally, from the measurements in Table 1 the water level was calculated to have decreased by 0.015m. Using these calculations and the time frame of the experiment the original evaporation rate was found to 0.50 ml/min. This was much lower than the uncontrolled water flow of 300 ml/min and was the reason the evaporation chamber was not running at steady state.

5.2 10/5/21 Initial Temperatures Experiment

Another experiment was run to determine how the heater is affecting the temperatures of the full system. Again, the operating procedure was followed to set up the system and 500ml of water were added to the evaporation chamber. The experiment was run for 0.65 days and temperature and humidity measurements were recording using GoVee hydrometers. From the the GoVee data seen in Figure 14 the temperatures of the chambers oscillated due to the heater is going through a duty cycle in order to maintain the water temperature at 40 °C.

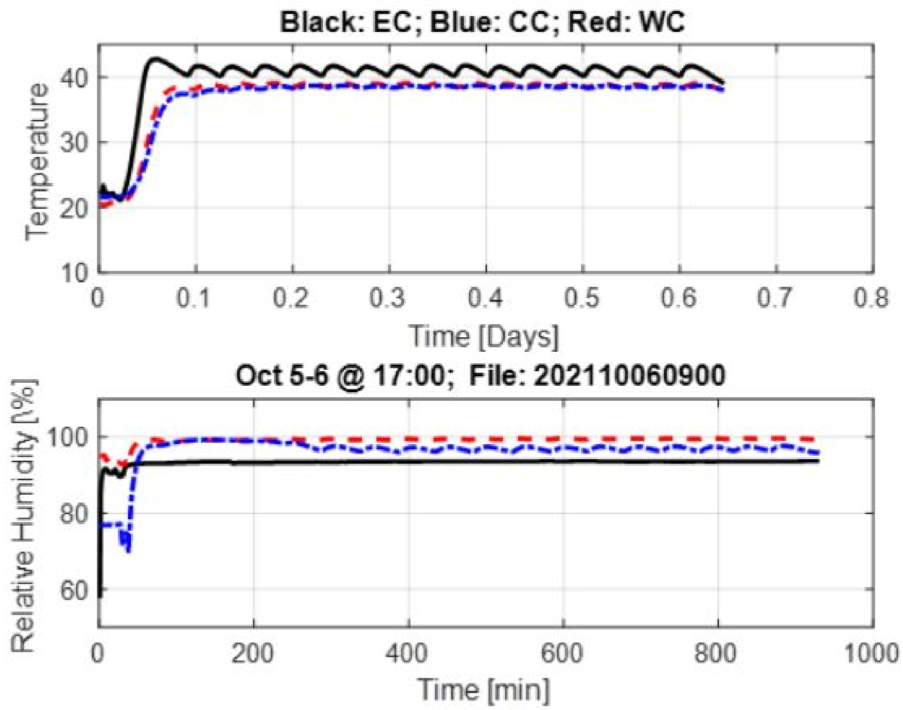

Figure 14. GoVee temperature and humidity data

From these two experiments it was clear that more controls and measurements were needed in order to determine how close to steady state the system was running. After the new Arduino/Raspberry Pi data collection system, water collection chamber, larger air pump, additional air stones, water level camera system, rewiring of safety cutoff circuity, water flow and air flow control rotameters, and power meter were added additional experiments were run.

5.3 11/4/21 Experiment with Design Changes

To test out all of the new design changes an experiment was following the operation procedure. The water inflow was set to 10 ml/min, the air flow rate was measured to be 80 LPM, and 350 ml of water was added to the evaporation chamber. The experiment was run for 18 hours.

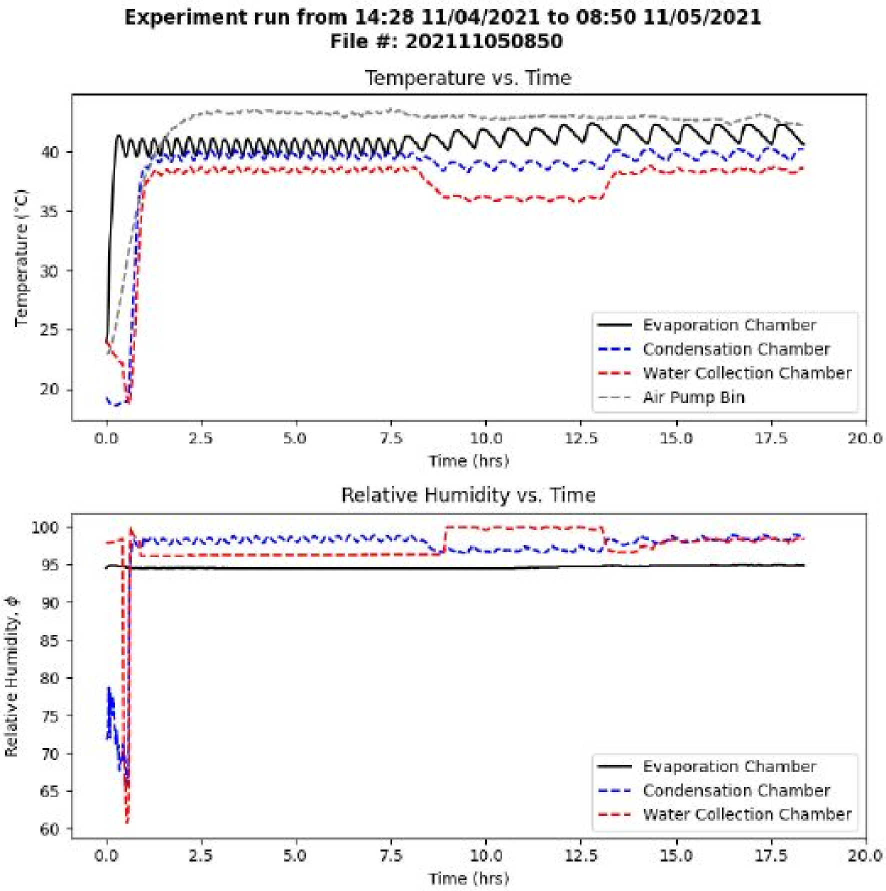

Figure 15. GoVee temperature and humidity data

From this experiment it was found that the water level of the evaporation chamber was not staying at a constant level and temperatures of the water collection chamber and condensation chamber were much higher than an expected. Additionally, as seen in Figure 15 and Figure 16 there was large heat input to the evaporation chamber besides the 500W heater which caused the temperatures to increase.

This additional heat source was found to be the air that was being pumped in through the air stones. The decision was made to implement a copper heat exchanger into the evaporation chamber for the inlet air before it entered the air stones. This heat exchanger directly heated the water and helped decrease the temperature inlet air before the air stones. Another experiment was run on 11/17/21 with the new copper heat exchanger

Figure 16. Arduino thermocouple data

following the same operational procedure as previous experiments. The analysis of this experiment is done in the Model and Experiment comparison section below.

6 Experiments and Comparison to Model

Data obtained from various experiments throughout the semester was used to validate the model and determine issues with the system.

6.1 Experiment Run on November 17th

A few experiments were run using the final design iteration of the system. For this experiment, three heat sources feed into the evaporation chamber: the 500W heater, the inlet water heated by the condenser, and the hot air (which adds heat to the system indirectly and directly via the copper coil and the air bubbles, respectively). This experiment also takes place before the fan is added to the duct between the evaporation and condensation chambers. The large air pump was used, providing 66 LPM of air. The water inflow rate was set at 4 mL/min following previous experimental data that showed that the steady-state evaporation rate was around 1-5 mL/min.

6.1.1 Results of Experiment

The experiment began on 11/17 at 13:50, and concluded on 11/18 at 11:10 (a full length of 21 hours, 20 minutes). After this time, the tank had filled up with 1677 mL of water. Additionally, the condenser system had collected 900 mL of water. These results give system values of

$$\text{Fill Rate} = \frac{1677\,\text{mL}}{1280\,\text{min}} = 1.31\,\text{mL/min}$$
$$\text{Evaporation Rate} = 4\,\text{mL/min} - 1.31\,\text{mL/min} = 2.69\,\text{mL/min}$$
$$\text{Condensation Rate} = \frac{900\,\text{mL}}{1280\,\text{min}} = 0.70\,\text{mL/min}$$

Temperature and relative humidity data was recorded by the thermocouples and Govee hygrometers. These results are shown in Figs. 17 and 18. Additionally, Table 2 shows average steady-state operating temperatures throughout the system for the experiment.

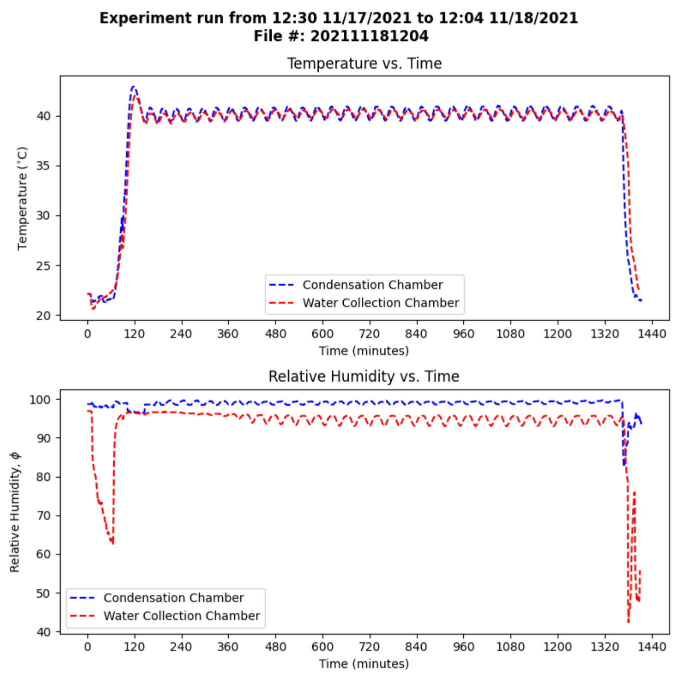

Figure 17. Govee data from the experiment run on 11/17, showing temperature and relative humidity; the Govee in the evaporation chamber is omitted because it failed, likely due to constant exposure to high humidity

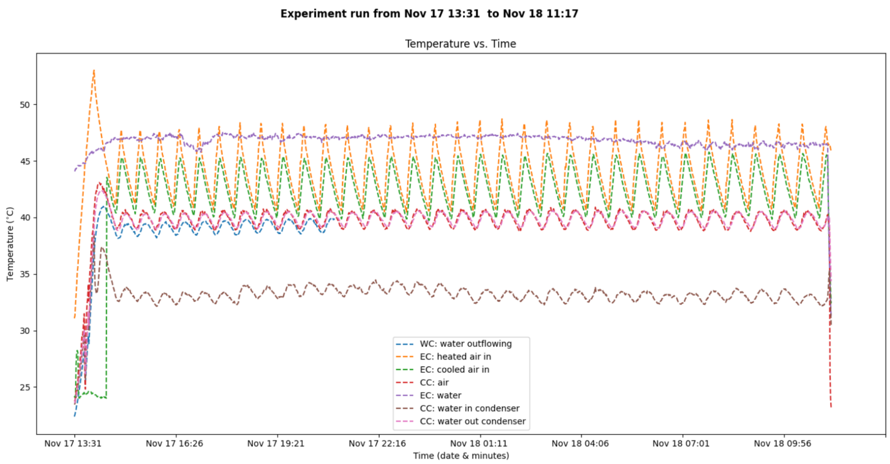

Figure 18. Thermocouple data from the experiment run on 11/17, showing temperature

Table 2. Average temperatures in different locations for the experiment run on 11/17, found using Fig. 18

Fluid & Location	**Average Temperature**
Air entering copper tubing	44.13°C
Air exiting copper tubing	42.66°C
Water in evaporation chamber	46.92°C
Water exiting condenser	39.85°C
Air in condensation chamber	39.88°C
Water leaving system (past condenser)	39.09°C

6.1.2 Application of the Model

Evaporation Chamber The following tables show the values of various parameters used to determine the heat needed from the heater to reach the evaporation rate of 2.69 mL/min. Given the relative humidity of 28.71% from the hygrometer of the ambient air that the air pump is utilizing, equations [1] and [2] provide the mass flow rate of dry air into the system from the moist ambient laboratory air. Theoretically, the mass flow rate of water vapor evaporating from the system should be equal to equation [9] with a relative humidity of 100%. This theoretical maximum evaporation rate given the air pump used is 3.31 mL/min.

Table 3. Volumetric Flow Rates

Parameter	*Experimental Value*
Incoming Water	4 mL/min
Air	66.7 L/min
Water Vapor	2.69 mL/min

Table 4. Mass Flow Rates

Parameter	*Experimental Value*
Incoming Water	6.647E-5 kg/s
Air	1.25E-3 kg/s
Water Vapor	4.919E-5 kg/s

Table 5. Enthalpies

Parameter	*Experimental Value*
Incoming Water	72.8 kJ/kg at 40°C
Air before copper tubing	317.7 kJ/kg at 44.15°C
Air after copper tubing and into system	316.1 kJ/kg at 42.63°C
Outgoing Air	321 kJ/kg at 47.5°C
Water Vapor	2588 kJ/kg

Substituting in the known values for equation [11] a heat input from the heater is determined as 94.7W. The experimentally determined heat input is 149.29W. This value was determined from inspecting the duty cycle of the heater while the experiment was performing in the pseudo steady state. The heater would output 550W for 27.14% of the whole experiment, resulting in 149.29W on average. This difference between the expected value of the model to the actual value experimental found is 36.57% which is viewed as the heat lost from the system.

6.1.2.1 Condensation Chamber The application of the model begins by calculating the air, water vapor, and simulated seawater mass flowrates, using Eqns. 16, 17, and 18 in combination with the humidity ratios before and after the open end of the condenser. Then, Eq. 19 can be rearranged to give

$$\dot{m}_w = \frac{\dot{m}_{sw}(h_{sw,i} - h_{sw,o}) + \dot{m}_a[\omega_i h_{v,i} + h_{a,i} - \omega_o h_{v,o} - h_{a,o}]}{h'_{fg} + c_{p,w}(T_{w,o} - T_{v,i})},$$

where the enthalpies and additional terms are found using Table A-2 and A-22 in [11] and Table A.4 and A.6 in [10]. The terms used in the calculation are shown in Table 6. The theoretical condensation rate using humidity ratios $\omega_o = 4.31\%$ and $\omega_i = 4.12\%$ is found to be

$$\dot{m}_w = 0.771\,\text{mL/min},$$

which is about 10% larger than the actual condensation rate determined experimentally. Because the model is applied to experimental conditions, this perceived loss in condensation is likely due to condensation on the walls of the condensation chamber, water collection chamber, and the tubing connecting to the gallon jug for water collection.

Table 6. Property values for the experiment run on 11/17

Property	**Value**
Seawater Volumetric Flowrate (mL/min)	4
Air Volumetric Flowrate (LPM)	6
Seawater Mass Flowrate (kg/s)	0.0000664667
Air Mass Flowrate (kg/s)	0.00128
$h_{sw,i}$ (kJ/kg)	235.13
$h_{sw,o}$ (kJ/kg)	262.24
$h_{v,i}$ (kJ/kg)	2574.30
$h_{v,o}$ (kJ/kg)	2541.70
$h_{a,i}$ (kJ/kg)	310.24
$h_{a,o}$ (kJ/kg)	290.16
h'_{fg} (kJ/kg)	2577.16
$c_{p,w}$ (kJ/(kg·K))	4.178
$T_{w,o}$ (°C)	20
$T_{v,i}$ (°C)	40

6.2 General Results

A number of experiments were run throughout the semester, but because the system was largely being improved upon and the model was in development, the experiments served a dual purpose of being used for the model and for motivating further design changes. Fig. 19 demonstrates that in general the design changes helped improve the evaporation rate of the system; this was to be expected, as some of the design changes included larger dry air inflow and more air stones (creating more bubbles, and more evaporation).

Some other important results can be derived from the experiments run throughout the semester. Looking at the Govee data in Fig. 20, it can be seen that the relative humidity of the condensation chamber is not much higher than that of the water collection chamber; at some points in the heater duty cycle, they are the same. This is quite alarming, as it means that conditions are relatively the same before and after the open end of the condenser. This issue is likely a result of the pursuit of steady-state conditions in the evaporation chamber—the water inflow rate was too low, and as such not enough heat could be taken out of the water vapor. Even though the system can potentially reuse some of the energy of the heater in the form of the latent heat of the vapor, it does not use this energy because of the bottleneck created by poor condensing conditions. To combat this it is recommended that more focus be put on the condenser chamber of the system, in

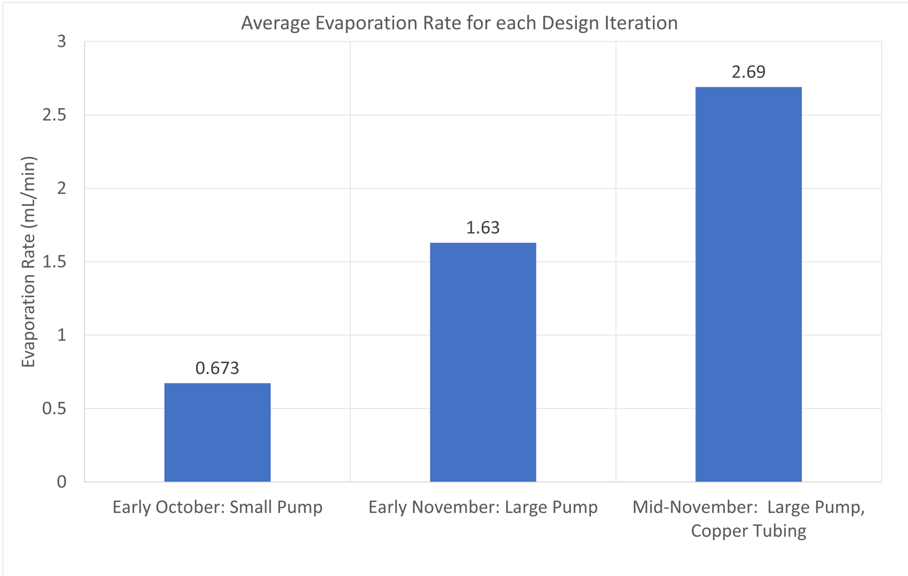

Figure 19. The system average evaporation rate from all experiments performed during each major design iteration

addition to the evaporation chamber.

Lastly, the system efficiency is defined as follows:

$$\text{System Efficiency}, \eta = \frac{\dot{m}_w h'_{fg}}{\text{Heater Power}},$$

where $\dot{m}_w$ is the condensation rate of the system and h'_{fg} is the modified latent heat of vaporization of the water. The system efficiency can be defined in a number of ways; however, this method treats the condenser as the system output, and the heater as the system input. From experiments run in November after the acrylic water chamber was installed, plugging in experimental values resulted in an average system efficiency of the system is around 18%. This result is quite low, but does show that at the very least the system is taking in water, evaporating it, and then condensing it; the process is feasible, and can be improved upon. This system efficiency value is likely an overestimate, as other power sources were not accounted for. These include the power going into the air pump and the condenser fans. This estimate of the system efficiency can be improved by increasing the water output of the system per the heater power input. Ways to improve this would include improving the condensation process and incorporating regeneration of

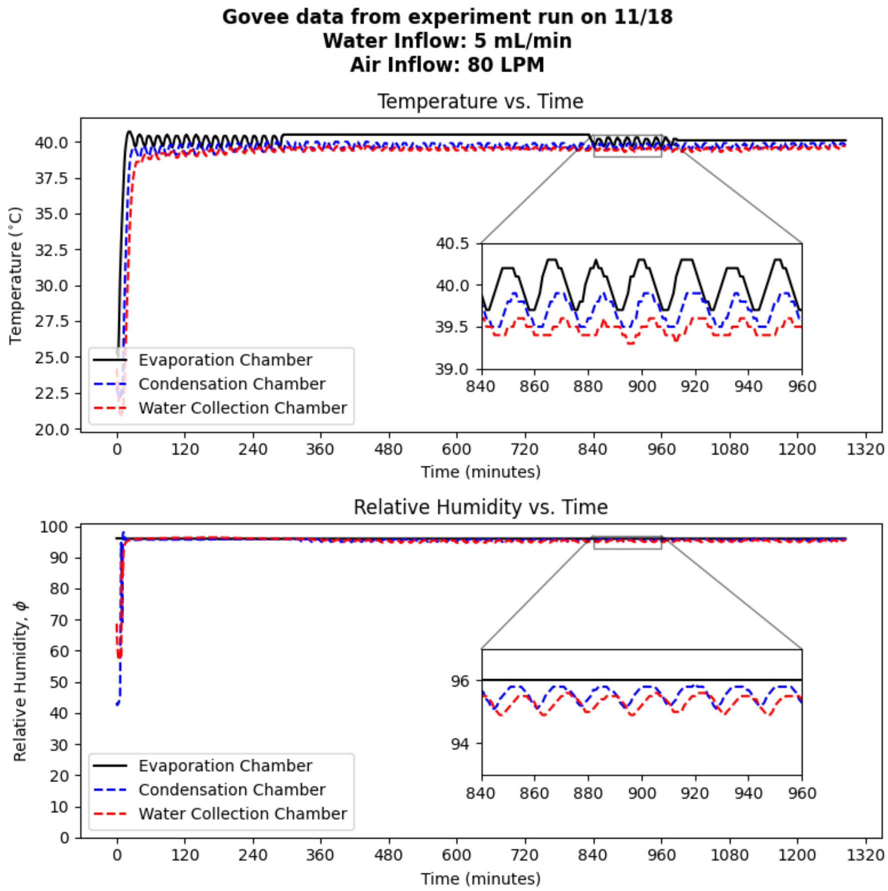

Figure 20. Govee temperature and relative humidity data from an experiment run on November 18th at 5 mL/min water inflow and 66 LPM

energy (which this efficiency value does not record).

7 Budget

Items were purchased using the $1500 budget to help supplement improving the desalination system. The majority of the cost associated with this semester's budget involved devices for data collection and control of the system's steady-state variables and the labor involved with the fabrication of the water collection chamber. The cost of these items were billed through the MechSE Business Office. The other costs are from the materials purchased at Innovation Studio and the cost of labor through the MechSE Machine Shop. As seen in Table 7, the total cost of system improvements made this semester was \$1079.52, so \$420.48 remains of the semester's budget.

Table 7. Final budget summary and itemized list

Budget Summary	
Total Spent: $1,079.52	
Category	**Total**
Allowance	1,500.00
Materials	51.43
Data Collection	497.09
Software	0.00
Transportation	0.00
Labor	531.00
Tools	0.00
Other	0.00

Itemized Budget List				
Category	**Description**	**Amount**	**Unit Cost**	**Total Price**
Allowance	Total Money Allotted	1.00	$1,500.00	$1,500.00
Materials	Needle Valve	1.00	$18.60	$18.60
Data Collection	REED Instruments Power Meter	1.00	$35.27	$35.27
Data Collection	Water Flowmeter	1.00	$77.05	$77.05
Data Collection	Air Pressure Gauge	1.00	$12.95	$12.95
Materials	3/8" Tee Junction	1.00	$12.83	$12.83
Data Collection	5 MP USB Camera	1.00	$75.73	$75.73
Data Collection	Amplifer MAX31856 Breakout	4.00	$17.50	$70.00
Data Collection	Raspberry Pi 4 Starter Kit	1.00	$105.00	$105.00
Materials	1/4" Acrylic Sheet	1.00	$20.00	$20.00
Materials	1/4" Acrylic Sheet	1.00	$0.00	$0.00
Materials	1/8" Acrylic Sheet	1.00	$0.00	$0.00
Labor	Water Collection Chamber	9.00	$59.00	$531.00
Data Collection	Wireless Keyboard & Mouse	1.00	$19.95	$19.95
Data Collection	HDMI 7" 800x480 Display	1.00	$79.95	$79.95
Data Collection	USB WI-FI dongle wifi	1.00	$9.21	$9.21
Data Collection	32GB SD Flash Memory Card	1.00	$11.98	$11.98

8 Conclusions and Recommendations

8.1 Accomplishments

The data collection systems of the solar desalination system were optimized and made for autonomous data collection at set rates. Pseudo-steady-state was achieved in the evaporation chamber, but required lower water input flowrates, which would in turn reduce the ability of the condenser to produce water condensate. A new water collection chamber was built that eliminated leaking and allowed for measurements of generated water to be made. Lastly, a model was constructed for the system that nearly matches the experimental results, with some minor differences.

8.2 Achieving Project Goals

The goals of the project were to reach steady state operating conditions of the evaporation and condensation chambers, implement design changes, and develop a thermodynamic model of the system. In order to meet these goals the an analysis of the initial prototype was conducted. From this analysis it was determined that improvements to system controls and measurements were needed, a new water collection chambered needed to be built, and an experiments needed to be run to find steady state with a correlating model. By having team members focus on different areas of improvement these changes were able to be made. Additionally, discussing experimental results and design changes with the project sponsor and advisor allowed for unknown problems to be found and possible solutions to be designed.

8.3 Changes to Project Objectives

Throughout the semester the overall project objectives did not change, however certain areas to focus on were altered. Initially, the focus of the project was to run experiments on the initial prototype. However, after these first experiments it was found that many design changes were needed in order to move towards steady state. This became the focus of a large portion of the project. Once these changes were made the focus shifted to matching experiments to modeling, which required fine tuning system inputs and data collection. With this new data the focus changed to evaluating problems with the condensation rate and designing possible solutions to fix this problem.

8.4 Recommendations

With steady state nearly achieved, next steps would be to include salt water, increase efficiency of individual processes, increase accuracy and precision of measuring devices, use a larger air pump, and introduce a control system for matching the condensation and evaporation rates of the system.

8.4.1 Increase Accuracy and Precision of Measuring Devices

One of the measuring devices that would benefit from being more precise is the rotameter controlling the inlet water mass flowrate. It is precise to 5mL/min, but the maximum evaporation rate, given the current air pump, is 3.31 mL/min. Being able to match this value is critical to achieving the steady state of the system.

Currently, a buoy switch system is used to turn off the water inflow into the system when the water level is too high and turn off the heater input into the system when the water level is too low. Additionally, a camera is used to capture the water level changes throughout experiments. However, to get a better control of the water level in the evaporation chamber a system should be designed that uses the water level measurements during an experiment to adjust the water flow to maintain the water level at a constant height.

8.4.2 Greater Air Inflow

The evaporation rate of the system is dependent on the mass air flow rate into the system. Increasing this value would in turn result in a higher evaporation rate. This value can be increased through the use of a more powerful air pump and a greater amount of air stones, which allow for more outlets the air can flow through.

8.4.3 Saltwater and Solar Power

In order to scale this system to industrial applications saltwater and solar power must be introduced to the system. The additional of solar power can be implemented to the system utilizing solar energy generated by solar panels to run the various power systems, which are currently plugged into wall outlets in the laboratory. Direct solar power had been utilized in previous semesters and was deemed insufficient. Saltwater can replace the fresh water currently in the system, however a system to remove the salt after the water is evaporated and prevent corrosion will need to be designed.

8.4.4 Interfacial Heating

In the future when the sun is introduced into this project, interfacial heating will be critical in evaporating the most water vapor from solar radiation. This method was discussed in our literature review. Currently the system uses bottom heating from an electric heater which is less efficient. When this system will be scaled in the future, maximizing the energy from solar radiation will be critical.

8.4.5 Improving Condensation

It is clear that the condenser is a bottleneck to the system, as the condensation and water collection chambers remain quite hot and humid throughout operation. There are multiple proposed ways to accomplish better condensation; however, the easiest way would be to increase the water mass flow rate through the condenser. This will provide more cold working fluid to perform the condensation with. Another alternative to increasing the water mass flow rate is discussed in the following section, and involves using a control system. A final alternative to either of these methods would be to completely change the condensation process. It may be possible to create a more simplified condenser by passing the chilled seawater through tubing through a chamber of hot water vapor with a basin to collect water at the bottom. Laminar film condensation would occur on the tubing. This would eliminate the need for two different chambers, while still incorporating regeneration of energy into the design.

8.4.6 Water Flow Control System

It is known from the condenser model that the condensation rate is increased by increasing the mass flow rate of water through the condenser. A high mass flow rate will keep the temperature of the water coming into the condenser at 10-15 °C and out of the condenser at about 34 °C as shown in experiment 12/4. However, a high water mass flow rate of water will overfill the evaporation chamber quickly. A control system should be implemented to provide a large water mass flow rate through the condenser, while providing a small water mass flow rate to match the evaporation rate in the evaporation chamber.

8.4.7 Modeling

It is apparent from experiments that the evaporation and condensation model should include quantifiable heat loss terms due to insufficient insulation; the effective insulation value of the system was investigated, but never fully calculated. Additionally, both models heavily rely on the fundamentals of thermodynamics, rather than incorporating any heat transfer effects. Some of the assumptions for the system are unrealistic, as is shown by the mismatch between model and experiments, and need to be explored further (such as estimating or calculating experimentally the effectiveness of the heat exchanger).

A Operating Manual

A.1 Electrical

There are many electrical components of the system that need power for operation such as the water cooler, water solenoid relay valve, raspberry pi, laptop, condenser-fan heat exchanger, circulation fan, power meter, air pump, and heater. Because all components need a voltage source for operation, power strips are required. To turn the system on, turn on switches of the power strips. Confirm everything is operating and plugged in. It is especially important to test the buoy switches for the water solenoid relay valve and heater located in the evaporation chamber. Actuate the buoys by hand and observe the heater thermometer turn on and off and the water solenoid valve shut off the water flow. It is crucial the switches work for an experiment to be run because they act as safety measures to shut off the water flow or turn off the heater if the water level in the evaporation chamber becomes too high or low.

A.2 Water Inflow

The water cooler must be plugged in and the water jug must have water to achieve water flow. The tubing is connected to the cold water outlet of the water cooler to represent the ocean temperature of about 12ºC. To control the water inflow, the red shut off valve located on the water cooler must be open, the blue shut off valve located along the tubing must be open, and the solenoid relay valve must also be open per its power source and buoy switch. The water flow rate can be manipulated by the needle valve; however, the rotameter provides a more precise adjustment by rotating its knob. The rotameter also gives an accurate measure of the water volumetric flow rate which can be observed by where the ball in the rotameter lines up with the measured marks on the device.

A.3 Heater

The heater must be plugged into the power meter to obtain an instantaneous power output reading. The heater must be placed underwater in the evaporation chamber to simulate the solar heat source to evaporate the water. The thermometer that controls the heat is secured in the air above the heated water, so the water vapor will have a temperature range of about 40ºC-42ºC. The heater turns off once the thermometer reads a temperature of 40°C, so the water temperature in the evaporation can be increased by moving the thermometer into the system vents or into the condensation chamber.

A.4 Air Inflow

The air pump must be plugged in to begin outputting air. Tubing must be connected from the barbed fitting of the air pump to the metal manifold located in the evaporation chamber. More tubing connects the air stones to the manifold. The air flow is varied by opening and closing the switches on the manifold that correlates to each air stone. The air volumetric flow rate is measured by connecting a rotameter to the tubing between the pump and the manifold.

A.5 Arduino Thermocouples Data

To begin gathering thermocouple data ensure that the Raspberry Pi power switch is on. If you are accessing the Raspberry Pi from a network other than IllinoisNet, a VPN connection to IllinoisNet must be turned on. Then log into Remote Desktop Connection application on your personal computer that comes standard with Windows operating systems (or the Microsoft Remote Desktop Connection application on IOS systems). Type in the Raspberry Pi IP addresses (10.194.147.106) into the computer line and the Raspberry Pi username (pi) into the username line. This will open a screen to login to the Raspberry Pi which has the same username and password (123) credentials. Next, open the terminal of the Raspberry Pi and type ”screen” (this will run a screen program allowing the remote desktop to close and still run the data program). Type ”python grabserial — ts ¿ ExperimentData.csv” (this will store the serial data in a csv format, the csv file name can be changed in this line to anything). To end the data collection type control C into the same line that started the program. Next, log into the WinSCP application on your personal computer and type in the same IP address and credentials as before to connect to the Raspberry Pi. The files stored on the Raspberry Pi will be shown on the right and your personal computer files will be shown on the left. Any experimental data csv files can then be directly dragged from the right screen (Raspberry Pi) to the left screen (your personal computer). These files can then plotted using the Python codes described below.

A.6 GoVee Hygrometers

GoVee hygrometers measure the temperature and humidity of their surroundings. They cannot be submerged in water, however, because the water will damage the circuitry and compromise the data collection. The data can be obtained via Bluetooth an app called GoVee Home. A phone can connect to the GoVee sensors where the data from a specific time can be chosen.

B Example of Using Sketchup Pro for Recording Water Level Measurements

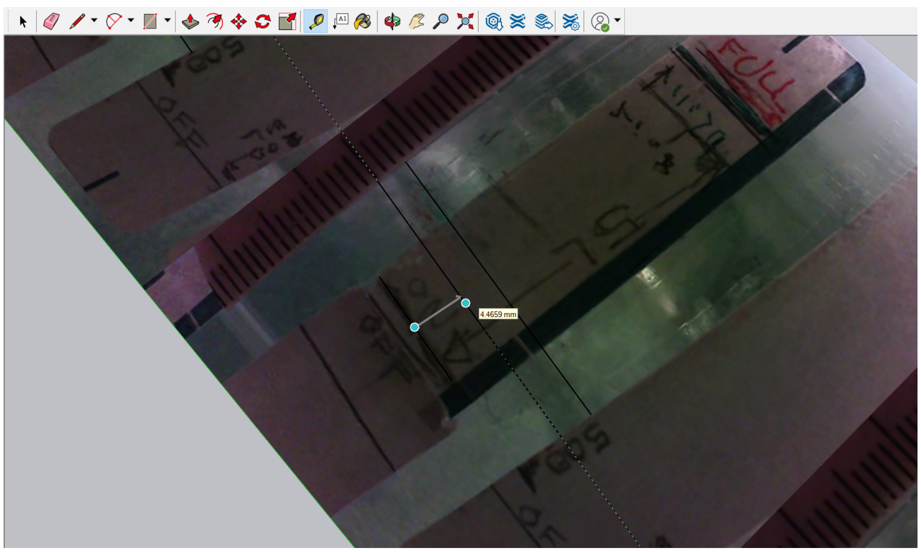

Figure 21. Recording water level

C Python Code for Operating Camera

```
import cv2
import time
import os

i = 0
Exp = 1
```

```
camera = cv2.VideoCapture(0) # 0 = Desktop camera, 1 = USB Camera
# Wait about 30 seconds and check if desktop camera light turns on, if so
    switch the index
# The index has flipped in the past

# Creating a new folder to store pictures
label = time.strftime("%a %b %d %Y", time.localtime())
while True:
    path = 'C:/Users/jontallen/PycharmProjects/pythonProject/{0} Experiment 
        {1}'.format(label, str(Exp))
    if not os.path.exists(path):
        os.makedirs(path)
        os.chdir(path)
        break
    else:
        Exp += 1

# Main code
while True:
    return_value, image = camera.read() # Takes a picture
    if image is None:
        print("Camera is not reading a picture, please check connection to 
            camera")
        print("Close all other applications using the camera")
        input("Restart the code")
    # gray = cv2.cvtColor(image,cv2.COLOR_BGR2GRAY)
    CheckMinute = time.strftime("%M", time.localtime())
    if CheckMinute in ['00', '05', '10','15','20','25','30','35','40','45','
        50','55']: # Input the minutes that you want the code to take a
        picture at
        for j in range(5):
            cv2.imwrite('WaterLevel'+str(i)+'_'+str(j)+'.jpg', image)
            print('Picture taken at {0}'.format(time.strftime("%c", time.
                localtime())))
            time.sleep(1)
            return_value, image = camera.read()
        i += 1
        time.sleep(60)
camera.release()
cv2.destroyAllWindows()
```

D Python Code for Graphing Thermocouple Data from Arduino

```
import matplotlib.pyplot as plt
import numpy as np
import pandas as pd
import os
import sys

"""
ArduinoDataGrab.py
--------------------------------
Reads Arduino Thermocouple Data
--------------------------------
"""

# ATTENTION: PASS THE NUMBER OF COLUMNS IN THE CSV (numCol)
# AND SET THE COLUMN NAMES (data.columns)

# Change the working directory to the one with the data. Most likely already
# the one you're using but just in case
os.chdir(r'C:\Users\wojta\Desktop\Fall 2021\Senior Project\Experiments\12_4')

# Assemble a list of all files in a specified folder
files = [filename for filename in os.listdir('.')]

# Pass the number of columns in the .csv file
numCol = 8

# Reads LAST csv file into pandas dataframes within the folder
for file in files:
    if '.csv' in file:
        data = pd.read_csv(file, header = 0, names= range(numCol))

# Get rid of second values
# data[0] = data[0].str.slice_replace(start = 12, stop = 15)

# # 11-17 specific, fixing faulty data
# data[1][16238:] = None

# Columns for Data
```

```
# 1) (yellow-green) EC: cooled air in
# 2) (yellow) EC: water
# 3) (red) WC: water out
# 4) (white) CC: water into condenser
# 5) (orange-blue) EC: heated air in
# 6) (orange) CC: water vapor
# 7) (blue) CC: water out condenser

# Consolidate relevant data into one dataframe
# It's up to the user to set these column names as they can change from
    experiment to experiment
if len(data.columns) == numCol:
    data.columns = ["Time","EC: cooled air in","EC: water","WC: water out","
        CC: water into condenser",
                    "EC: heated air in","CC: water vapor","CC: water out 
                        condenser"]

# Removes measurements made within the same minute
data = data.drop_duplicates(subset=["Time"])

# Create a plot
fig, axes = plt.subplots(1,1, figsize = (8,8))

# Plot the temperature vs. time data
for Col in data.columns[1:]:
    data[Col] = pd.to_numeric(data[Col], downcast="float")
    axes.plot(data["Time"], data[Col], ls = 'dashed', label = Col)

# x-tick mark adjustments
data_length = len(data)
dl_rem = data_length % 100
axes.set_xticks(np.linspace(0, data_length + (100 - dl_rem), 9)) # Labels
    data up to the next hundreds value after the data length

axes.set_xlabel("Time (date & minutes)")
axes.set_ylabel(r"Temperature ($^{\circ}$C)")
axes.legend()
# axes.legend(loc='center left', bbox_to_anchor=(1, 0.5))
axes.set_title("Temperature vs. Time")

# Set up title of subplots including file info
```

```
start_date_str = data["Time"][0]
end_date_str = data["Time"].iloc[-1]
plt.suptitle("Experiment run from %s to %s\n" % (start_date_str, end_date_str
    ), weight = "bold")

plt.tight_layout() # Necessary to keep text from overlapping
plt.show()
```

E Python Code for Evaporation Model

```
import numpy as np

# Initial Values
V_dot = {
    "water_in": 4, # mL/min
    "moist_air_in": 66.7, # L/min
    "vapor_out": 2.69, # mL/min
}

m_dot = {
    "water_in": 0,
    "dry_air": 0,
    "vapor_in": 0,
    "vapor_out": 0,

    "vapor_ratio": 0,
    "air_ratio": 0
}

h = {
    "water": 188.45, # kJ/kg at 45 C subcooled
    "air_heated_in": 315.27, # kJ/kg at 42.04 C
    "air_cooled_in": 314.15, # kJ/kg at 40.74 C
    "vapor_heated_in": 2577.93, # kJ/kg at 42.04 C
    "vapor_cooled_in": 2575.62, # kJ/kg at 40.74 C
    "air_out": 321, # kJ/kg at 47.5 C
    "vapor_out": 2588, # kJ/kg at 47.5 C
}

Q_dot = {
    "heater": 0,
```

```
    "heater_ratio_v": 0,
    "heater_ratio_a": 0,
    "air": 0
}

ro = {
    "water": 997, # kg/m^3
    "air": 1.127, # kg/m^3
    "saturated_vapor": 0.05122 # kg/m^3
}

# Converting
V_dot["moist_air_in"] /= 6E4 # m3/s

V_dot["water_in"] /= 6E7 # m3/s
m_dot["water_in"] = V_dot["water_in"] * ro["water"] # kg/s

V_dot["vapor_out"] /= 6E7 # m3/s
m_dot["vapor_out"] = V_dot["vapor_out"] * ro["water"] # kg/s
""" We use the density of water above because we are converting the volume of
    water evaporated per unit of time to the mass flow rate of water vapor
    """

#
    ------------------------------------------------------------------------------

# Calculating mass flowrate of vapor and dry air going into the control
    volume
Relative_Humidity = {
    "11_29_Incoming": .2871, # %
}

Saturated_Water_Vapor_Pressue = {
    "23_C" : 0.02810 # bar
}

Atm_pressure = 0.9869 # bar

p_v = Relative_Humidity["11_29_Incoming"] * Saturated_Water_Vapor_Pressue["23
    _C"] # barr
Humidity_Ratio = 0.622 * (p_v/(Atm_pressure-p_v)) # kg (vapor) / kg (dry air)
```

```
m_dot["dry_air"] = V_dot["moist_air_in"]/((Humidity_Ratio/ro["saturated_vapor
    "])+(1/ro["air"])) # kg/s
m_dot["vapor_in"] = Humidity_Ratio*m_dot["dry_air"]

#
    ------------------------------------------------------------------------------

# 100% Humidity ratio theoretical values
m_dot["vapor_ratio"] = m_dot["dry_air"] * 0.04889 # kg/s
m_dot["air_ratio"] = m_dot["vapor_out"] / 0.04889 # kg/s

#
    ------------------------------------------------------------------------------

# Checking stuff
print("mass flowrates of water and vapor in = {0}".format(m_dot["vapor_in"] +
     m_dot["water_in"]))
print("mass flowrate of vapor out = {0}".format(m_dot["vapor_out"]))

print(m_dot)

#
    ------------------------------------------------------------------------------

# Governing Equation
# 0 = Q_heater + Q_air +    (m_i*hi) -    (m_e*h_e)
# 0 = Q_heater + Q_air + m_wi*h + m_ai*h + m_vi*h - m_ao*h - m_vo*h
Q_dot["air"] = m_dot["dry_air"] * (h["air_heated_in"]-h["air_cooled_in"]) +
    m_dot["vapor_in"] * (h["vapor_heated_in"]-h["vapor_cooled_in"])

Q_dot["heater"] = m_dot["vapor_out"]*h["vapor_out"] + m_dot["dry_air"]*h["
    air_out"] - Q_dot["air"] - m_dot["dry_air"]*h["air_cooled_in"] - m_dot["
    vapor_in"] * h["vapor_cooled_in"] - m_dot["water_in"]*h["water"]
# Q_dot["heater_ratio_v"] = m_dot["vapor_ratio"]*h["vapor_out"] + m_dot["
    dry_air"]*h["air_out"] - Q_dot["air"] - m_dot["dry_air"]*h["air_cooled_in
    "] - m_dot["water_in"]*h["water"]
# Q_dot["heater_ratio_a"] = m_dot["vapor_in"]*h["vapor_out"] + m_dot["
    air_ratio"]*h["air_out"] - Q_dot["air"] - m_dot["air_ratio"]*h["
    air_cooled_in"] - m_dot["water_in"]*h["water"]
print(Q_dot)
```

F Arduino Thermocouple Code

```
//include neccesary libraries
#include <Adafruit_MAX31856.h>

// Use software SPI: CS, DI, DO, CLK
Adafruit_MAX31856 maxthermo1 = Adafruit_MAX31856(29, 27, 25, 23);
Adafruit_MAX31856 maxthermo2 = Adafruit_MAX31856(37, 35, 33, 31);
Adafruit_MAX31856 maxthermo3 = Adafruit_MAX31856(45, 43, 41, 39);
Adafruit_MAX31856 maxthermo4 = Adafruit_MAX31856(53, 51, 49, 47);
Adafruit_MAX31856 maxthermo5 = Adafruit_MAX31856(22, 24, 26, 28);
Adafruit_MAX31856 maxthermo6 = Adafruit_MAX31856(30, 32, 34, 36);
Adafruit_MAX31856 maxthermo7 = Adafruit_MAX31856(38, 40, 42, 44);

void setup() {
  Serial.begin(9600);
  while (!Serial) delay(10);
  Serial.println("MAX31856 thermocouple test");

  //starting data collection for each sensor
  maxthermo1.begin();
  maxthermo2.begin();
  maxthermo3.begin();
  maxthermo4.begin();
  maxthermo5.begin();
  maxthermo6.begin();
  maxthermo7.begin();

  //setting thermocouple type
  maxthermo1.setThermocoupleType(MAX31856_TCTYPE_K);
  maxthermo2.setThermocoupleType(MAX31856_TCTYPE_K);
  maxthermo3.setThermocoupleType(MAX31856_TCTYPE_K);
  maxthermo4.setThermocoupleType(MAX31856_TCTYPE_K);
  maxthermo5.setThermocoupleType(MAX31856_TCTYPE_K);
  maxthermo6.setThermocoupleType(MAX31856_TCTYPE_K);
  maxthermo7.setThermocoupleType(MAX31856_TCTYPE_K);
}

void loop() {
  Serial.print(", ");
  Serial.print(maxthermo1.readThermocoupleTemperature());
```

```
  Serial.print(", ");
  Serial.print(maxthermo2.readThermocoupleTemperature());
  Serial.print(", ");
  Serial.print(maxthermo3.readThermocoupleTemperature());
  Serial.print(", ");
  Serial.print(maxthermo4.readThermocoupleTemperature());
  Serial.print(", ");
  Serial.print(maxthermo5.readThermocoupleTemperature());
  Serial.print(", ");
  Serial.print(maxthermo6.readThermocoupleTemperature());
  Serial.print(", ");
  Serial.print(maxthermo7.readThermocoupleTemperature());
  Serial.print("\n");

  delay(500);

}
```

G Additional Photos of the System

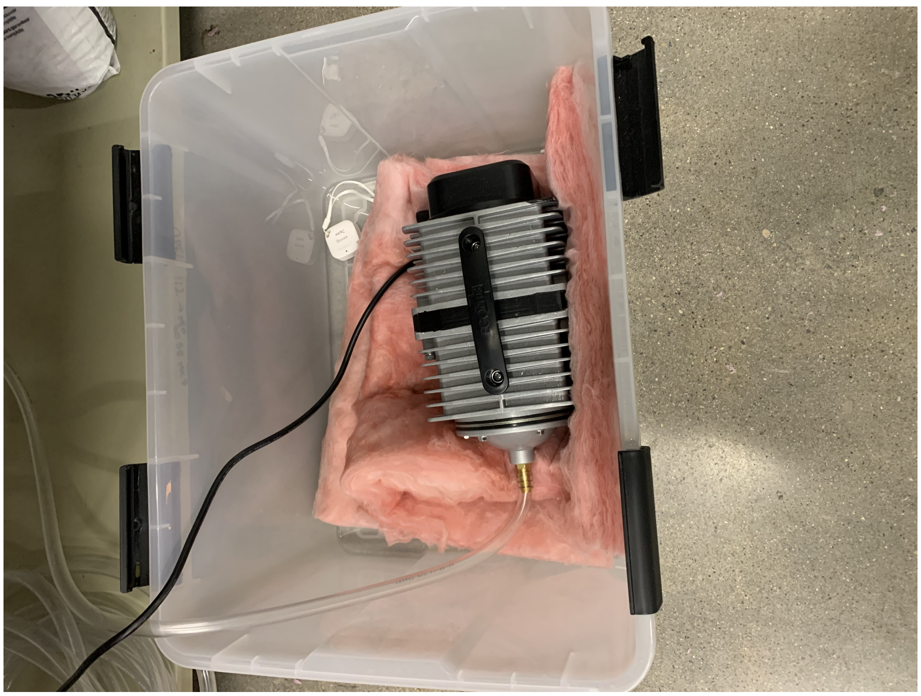

Figure 22. 66 LPM air pump used in experimentation; the pump was placed in a container with fiberglass insulation to dampen noise output

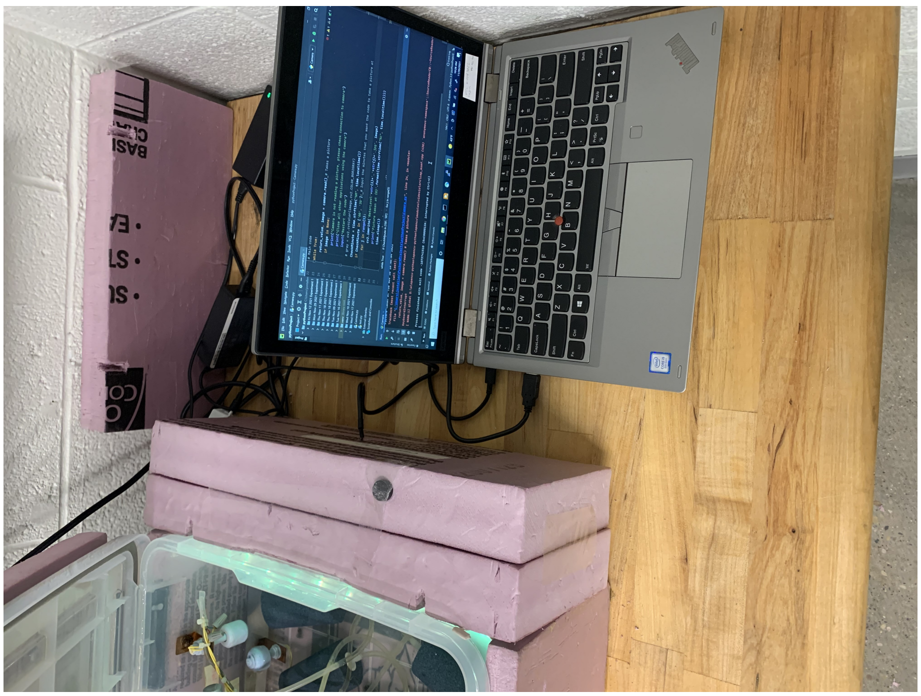

Figure 23. Camera system to autonomously measure water level of the system

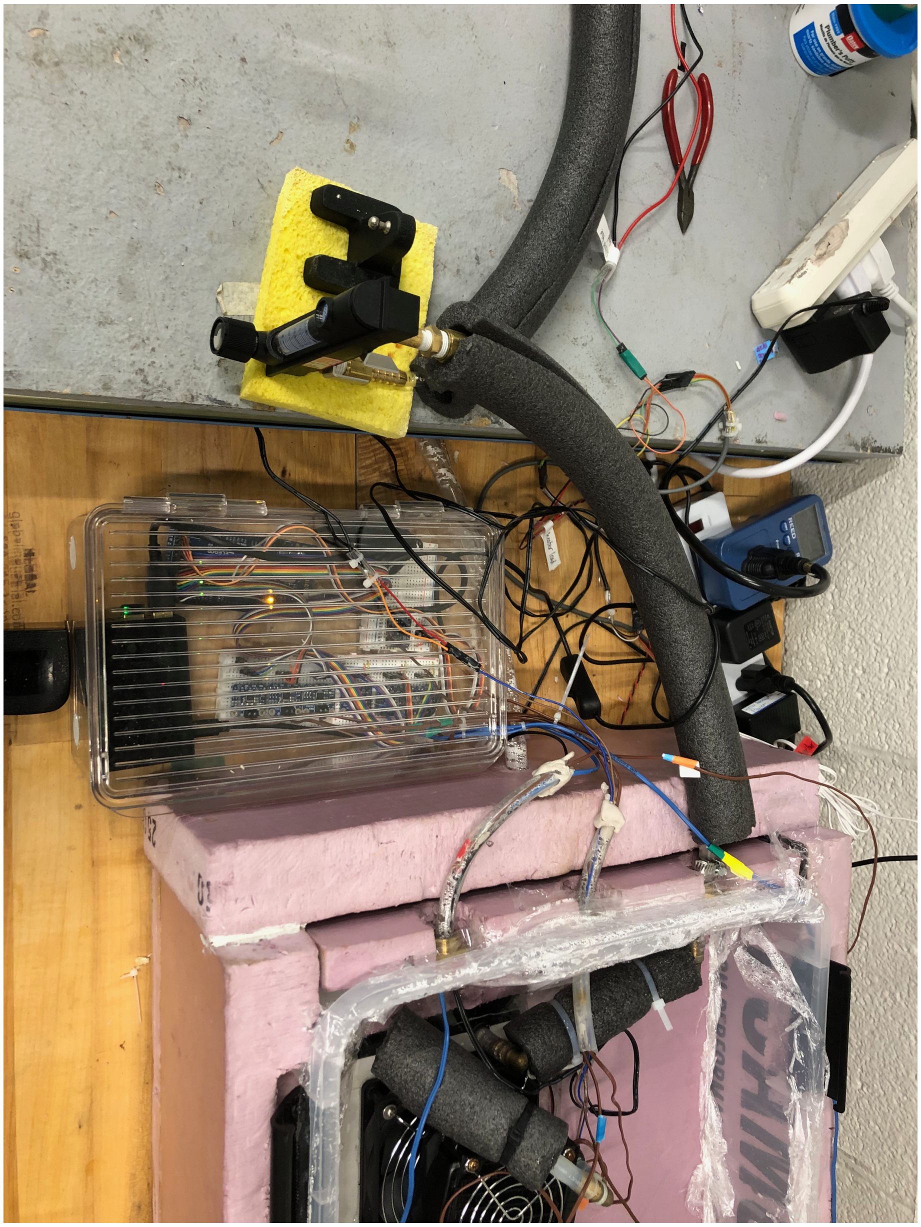

Figure 24. Arduino/Raspberry Pi data collection system being used with thermocouples

References

[1] E. Kabir, P. Kumar, S. Kumar, A. A. Adelodun, and K.-H. Kim, "Solar energy: Potential and future prospects," *Renewable and Sustainable Energy Reviews*, vol. 82, pp. 894–900, 2018. [Online]. Available: https://www.sciencedirect.com/science/article/pii/S1364032117313485

[2] T. Shedd and T. Newell, "An automated optical liquid film thickness measurement method," *UIUC*, pp. 1–78, 1997, measuring depth of water using laser refraction and reflection. [Online]. Available: https://aip.scitation.org/doi/10.1063/1.1149232

[3] P. Tao, G. Ni, C. Song, W. Shang, J. Wu, J. Zhu, G. Chen, and T. Deng, "Solar-driven interfacial evaporation," *Nature Energy*, pp. 1031–1041, 2018, interfacial Evaporation. [Online]. Available: https://www.nature.com/articles/s41560-018-0260-7

[4] "Nasa: Climate change and global warming," 2021. [Online]. Available: https://climate.nasa.gov/

[5] A. Etemadi, A. Emdadi, O. AsefAfshar, and Y. Emami, "Electricity generation by the ocean thermal energy," *Energy Procedia*, vol. 12, pp. 936–943, 2011, the Proceedings of International Conference on Smart Grid and Clean Energy Technologies (ICSGCE 2011. [Online]. Available: https://www.sciencedirect.com/science/article/pii/S1876610211019497

[6] Y. Wang, S. Wu, Y. Yang, X. Yang, H. Song, Z. Cao, and Y. Huang, "Evaporation and movement of fine droplets in non-uniform temperature and humidity field," *Building and Environment*, vol. 150, pp. 75–87, 2019. [Online]. Available: https://www.sciencedirect.com/science/article/pii/S0360132319300034

[7] H. Jaakola, "Cost effective evaporators for desalination," *Desalination*, vol. 108, pp. 357–360, 1997. [Online]. Available: https://www-sciencedirect-com.proxy2.library.illinois.edu/science/article/pii/S0011916497000441#aep-abstract-id4

[8] A. M. Abdel Dayem, "Efficient Solar Desalination System Using Humidification/Dehumidification Process," *Journal of Solar Energy Engineering*, vol. 136, no. 4, 06 2014, 041014. [Online]. Available: https://doi.org/10.1115/1.4027725

[9] S. Al-Kharabsheh and D. Y. Goswami, “Theoretical Analysis of a Water Desalination System Using Low Grade Solar Heat ,” *Journal of Solar Energy Engineering*, vol. 126, no. 2, pp. 774–780, 05 2004. [Online]. Available: https://doi.org/10.1115/1.1669450

[10] T. L. Bergman and A. S. Lavine, *Fundamentals of Heat and Mass Transfer, 8th Edition*. Hoboken, NJ: John Wiley & Sons, Inc., 2017.

[11] M. Moran, H. Shapiro, D. Boettner, and M. Bailey, *Fundamentals of Engineering Thermodynamics, 8th Edition*. New York, NY: John Wiley & Sons, Inc., 2014.